Running title: Sugar beet raffinose metabolism

Cold-triggered induction of ROS- and raffinose-related metabolism in freezing-sensitive taproot tissue of sugar beet

Isabel Keller[1], Christina Müdsam[2], Cristina Martins Rodrigues[1], Dominik Kischka[2], Wolfgang Zierer[2], Uwe Sonnewald[2], Karsten Harms[3], Olaf Czarnecki[4], Karin Fiedler-Wiechers[4], Wolfgang Koch[4], H. Ekkehard Neuhaus[1], Frank Ludewig[4], Benjamin Pommerrenig[1*]

Corresponding Author:

Dr. Benjamin Pommerrenig
Plant Physiology
University of Kaiserslautern
Paul-Ehrlich-Str 22
67663 Kaiserslautern
Germany
Phone: +49 (0) 631 2052894
E-Mail: pommerre@bio.uni-kl.de

[1]Department of Plant Physiology, University of Kaiserslautern, Paul-Ehrlich-Str.22, 67663 Kaiserslautern, Germany
[2]Department of Biochemistry, FAU Erlangen-Nürnberg, Staudtstr. 5, 91052 Erlangen, Germany
[3] Südzucker AG, CRDS, Wormser Str. 11, 67283 Obrigheim/Pfalz, Germany
[4]KWS SAAT SE & Co. KGaA, Grimsehlstraße 31, 37574 Einbeck, Germany

Short title: Sugar beet raffinose metabolism

1

1 **Abstract**

2   Sugar beet (*Beta vulgaris subsp. vulgaris*) is the exclusive source of sugar in the form of sucrose in

3   temperate climate zones. There, sugar beet is grown as an annual crop from spring to autumn because

4   of the damaging effect of freezing temperatures to taproot tissue. Natural and breeded varieties

5   display variance in the degree of tolerance to freezing temperatures and genotypes with elevated

6   tolerance to freezing have been isolated. Here we compare initial responses to frost between

7   genotypes with either low and high winter survival rates. The selected genotypes differed in the

8   severity of frost injury. We combined transcriptomic and metabolite analyses of leaf- and taproot

9   tissues from such genotypes to elucidate mechanisms of the early freezing response and to dissect

10   genotype- and tissue-dependent responses. Freezing temperatures induced drastic downregulation

11   of photosynthesis-related genes in leaves but upregulation of genes related to minor carbohydrate

12   metabolism, particularly of genes involved in raffinose metabolism in both, leaf and taproot tissue. In

13   agreement with this, it has been revealed that raffinose and the corresponding intermediates, inositol

14   and galactinol, increased markedly in these tissues. We found that genotypes with improved tolerance

15   to freezing, showed higher accumulation of raffinose in a defined interior region within the upper

16   part of the taproot, the pith, representing the tissue most susceptible to freeze damages. This

17   accumulation was accompanied by specific upregulation of raffinose synthesizing enzymes in

18   taproots, suggesting a protective role for raffinose and its precursors for freezing damage in sugar

19   beet.

20

21

22 **INTRODUCTION**

23 In temperate climate zones (Europe and North America), sugar beet (*Beta vulgaris subsp. vulgaris*) is

24 the exclusive source of sugar (sucrose) for the food industry and a source for bio-energy generation.

25 Sugar beet taproots are able to accumulate sucrose to up to nearly 20% of their fresh weight at

26 maturity (Dohm et al., 2013) and provide about 30% of the total sugar produced worldwide (Y.-F.

27 Zhang et al., 2017). Owing to its biennial lifestyle, the plant forms the huge sucrose-storing taproot

28 during the first year of its life cycle. The stored sugar is used to fuel the outgrowth of a flowering seed

29 stalk in the reproductive phase in the second year of growth (Chen et al., 2016). Induction of

30 flowering, however, requires a prolonged exposure to cold (between 5-20 weeks at 4-15°C), known

31 as vernalization (Abo-Elwafa et al., 2006; Kockelmann et al., 2010). During vernalization, shoots and

32 taproots prepare for metabolic and functional rearrangements resulting in a switch of their source

33 and sink identities, where shoot metabolism depends on carbon supply from the taproot to allow

34 outgrowth of the seed stalk (Rodrigues et al., 2020). Successful vernalization of sugar beet plants can

35 only occur at low, but above-zero temperatures. This is because, despite the high accumulation of

36 sugars, which are known to stabilize membranes and protect against freezing-induced damages

37 (Anchordoguy et al., 1987; Pommerrenig et al., 2018), sugar beet is sensitive to subzero temperatures

38 (Barbier et al., 1982; Loel and Hoffmann, 2015). This sensitivity allows cultivation of the crop in its

39 production area only in a limited vegetation period from spring to late autumn. The limited growth

40 period and the slow formation of leaves in spring are its main yield limiting factors (Jaggard et al.,

41 2009; Milford and Riley, 1980). Calculations taking an increased freezing and bolting tolerance into

42 account suggested that an elongated growth period of sugar beet might result in an increase of the

43 total sugar yield by about 25% (Hoffmann and Kluge-Severin, 2011). However, overwintering sugar

44 beet plants must be able to withstand freezing temperatures, and therefore, freezing tolerance has

45 become a desirable trait for sugar beet breeders. Freezing temperatures frequently lead to severe

46 yield losses of different crops (Barbier et al., 1982; Chang et al., 2014; Fennell, 2004; Maqbool et al.,

3

47   2010), as intra- and extracellular ice formation damages plant tissue by rupturing cell membranes or

48   because of cellular dehydration (Burke et al., 1976; Wolfe and Bryant, 1999). On the macroscopic

49   level, the impact of freezing on sugar beet taproot tissue is drastic and results in lethal damage to

50   internal tissue and ultimately, the entire plant. Ice formation and thawing leads to cell rupture and

51   leakage of root sap, which ultimately attracts microorganisms and leads to rot of the taproot body

52   (Barbier et al., 1982).

53   Factors protecting plants against freezing may be soluble sugars, amino acids, organic acids, or

54   derivatives thereof, which function as osmolytes and can thus lower the freezing point, or prevent

55   cellular dehydration upon freezing. Additionally, some of these metabolites can stabilize enzymes,

56   membranes and other cellular components (Guy, 1990; Yadav, 2010). In particular, small

57   carbohydrates like fructans or raffinose family oligosaccharides (RFOs) have superior membrane

58   protective abilities and additionally represent potent quenchers of reactive oxygen species (ROS) (De

59   Roover et al., 2000; Hincha et al., 2007; Pontis, 1989). Accumulation of high levels of fructans in plants

60   of the Asteraceae familiy like chicory (*Cichorium intybus*) or Jerusalem artichoke (*Helianthus*

61   *tuberosus*), for example, render these species highly tolerant against freezing damage. Sugar beet does

62   not produce fructans but can form considerable amounts of raffinose, which are derived from sucrose,

63   especially during storage of taproots (Haagenson et al., 2008; Wyse and Dexter, 1971). However,

64   raffinose biosynthesis is attended by reduction of sucrose levels. In fact, as part of the so-called

65   molasses, raffinose is considered an unwanted contaminant lowering the maximum amount of

66   sucrose extractable from the pulp during industrial processing (Ganter et al., 1988; Wyse and Dexter,

67   1971). On the other hand, raffinose is important for plant frost tolerance (Nishizawa et al., 2008;

68   Pennycooke et al., 2003; Peters and Keller, 2009). Raffinose is a trisaccharide consisting of sucrose

69   and galactose and is synthesized via a subsequent transfer of activated galactose moieties, donated

70   by galactinol, to sucrose (Sengupta et al., 2015). Two specific enzymes, galactinol synthase (GOLS)

71   and raffinose synthase (RS), mediate the synthesis of galactinol and raffinose, respectively. GOLS

72   mediates the first metabolic step in raffinose biosynthesis, the conversion of UDP-Galactose and myo-

73   inositol to galactinol. Raffinose biosynthesis is specifically upregulated during cold acclimation

74   processes, and several galactinol synthase genes (*GOLS*) are transcriptionally regulated in *Arabidopsis*

75   *thaliana* via low temperature response transcription factors of the C- repeat binding factor (CBF)

76   family (Fowler and Thomashow, 2002; Gilmour et al., 2000; Taji et al., 2002). CBF proteins directly

77   regulate cold-responsive (COR) genes, which facilitate the acquisition of cold acclimation and

78   sustained freezing tolerance, as products of COR genes are involved in processes like the synthesis of

79   osmo-protectants and also raffinose, lipid metabolism or cell wall modification (Liu et al., 2019;

80   Thomashow, 1999). In sugar beet, CBFs like CBF3, were shown to be upregulated early upon cold and

81   freezing temperatures, but were only detected in roots so far (Moliterni et al., 2015).

82   In this work, we analyzed how low temperatures would influence the accumulation of diverse sugar

83   and RFO species in different sugar beet tissues and genotypes. In addition, we present detailed

84   information on raffinose- and inositol-related gene expression and substrate contents in different

85   organs and tissues of sugar beets, exposed to control and freezing temperatures. Our analysis

86   indicates that inositol and raffinose biosynthesis are spatially regulated in a low temperature-

87   dependent manner. We discuss whether these compounds could serve as indicators for the cold and

88   freezing stress level, or whether they may play a direct role in freeze-protection. The identified frost

89   protective substances represent possible targets for screening, breeding or genetic modification of

90   sugar beet varieties with increased winter hardiness and frost tolerance.

91   **RESULTS**

92   **Sugar beet genotypes respond differently to freezing temperatures**

93   Sub-zero temperatures have a detrimental effect on sugar beet tissue resulting in a structural collapse

94   of the affected cells leading to sucrose leakage out of vacuoles and eventual rotting of taproot tissue

95   (Barbier et al., 1982). To learn about physiological and molecular responses that might mitigate

96   harmful effects of freezing temperatures, we analyzed three genotypes (GT1, GT2, GT3) with different

97   freezing sensitivities from a panel of accessions that was tested for survival of freezing temperatures

98   in field or greenhouse trials. In these tests, GT1 had low survival rates (SR) (14% in field and 11% in

99   greenhouse trials), GT2 high SR (90% in field and 66% in greenhouse trials), and GT3 intermediate

100   SR (77% in field and 56% in greenhouse trials). These rates categorized GT1 as freezing sensitive,

101   GT2 as freezing tolerant, and GT3 as moderately freezing tolerant (**Fig. 1A**). For the experiments

102   presented in this paper, we grew the three different genotypes under a fixed temperature profile in

103   climate-controlled growth chambers and monitored their behavior in respect to the set temperature

104   (**Fig. 1B**). Freezing stress was applied until the temperature, measured 5 cm below the surface of the

105   potting soil, was decreased to 0°C (approximately 3 days). After frost exposure, plants were

106   transferred to 20°C for recovery. The severity of injuries by the three genotypes following treatment

107   indeed mirrored their survival rates from the prior field and greenhouse trials. For instance, most of

108   GT1 shoots collapsed during cold exposure and a comparably high number of GT1 plants did not

109   recover and died after the freezing treatment (**Fig. 1C**). Importantly, initial exposure to freezing

110   temperature did not kill plants, but severely affected their performance during recovery at higher

111   temperatures in a genotype-dependent manner (**Fig. 1C**). Photosynthesis, measured as effective

112   quantum yield of photosystem II (Φ_{II}), significantly declined at 0°C in all three genotypes, but

113   strongest in freezing-sensitive GT1 plants (**Fig. 1D**). In contrast, plants from the more freezing-

114   tolerant GT2 and GT3 genotypes were able to increase Φ_{II} to pre-freezing levels after retransfer to

115   12°C (**Fig. 1D**). Consistently, GT1 plants showed higher non-photochemical quenching (NPQ) in

116   comparison to GT2 and GT3 plants during and after exposure to frost (**Fig. 1D**).

117   Following treatment, a large number of roots from GT1 plants, displayed visible brownish rot in a

118   defined region within the taproot neck, designated as pith (**Fig. 1E**). With progression of the rotting,

119   affected taproots lost structural integrity and plants died. The pith tissues of the two more tolerant

120   cultivars, GT2 and GT3, were not affected to the same extent. Such changes, as observed above, can

121   be evoked by reactive oxygen species (ROS). To check whether the low temperature exposure was

122   associated with formation of ROS, we performed staining of taproot slices with diaminobenzidine

123   (DAB) and nitroblue tetrazolium (NBT) to reveal accumulation of H_2O_2 and superoxide, respectively.

124   Staining was most intense during or after freezing treatment and DAB-derived dark brown or NBT-

125   derived blue staining indicated that both types of reactive oxygen species strongly accumulated in the

126   vasculature and in the pith of taproots **(Fig. 1F and Supplemental Fig. S1A)**. Overall, our

127   observations revealed that frost induced tissue damage, as well as emergence of ROS are clustered in

128   the upper part of the sugar beet taproot, mainly in the pith tissue.

129
130
131
132

A

Geno-type	SR field	SR growth chamber
GT1	14%	11%
GT2	90%	66%
GT3	77%	56%

B

C
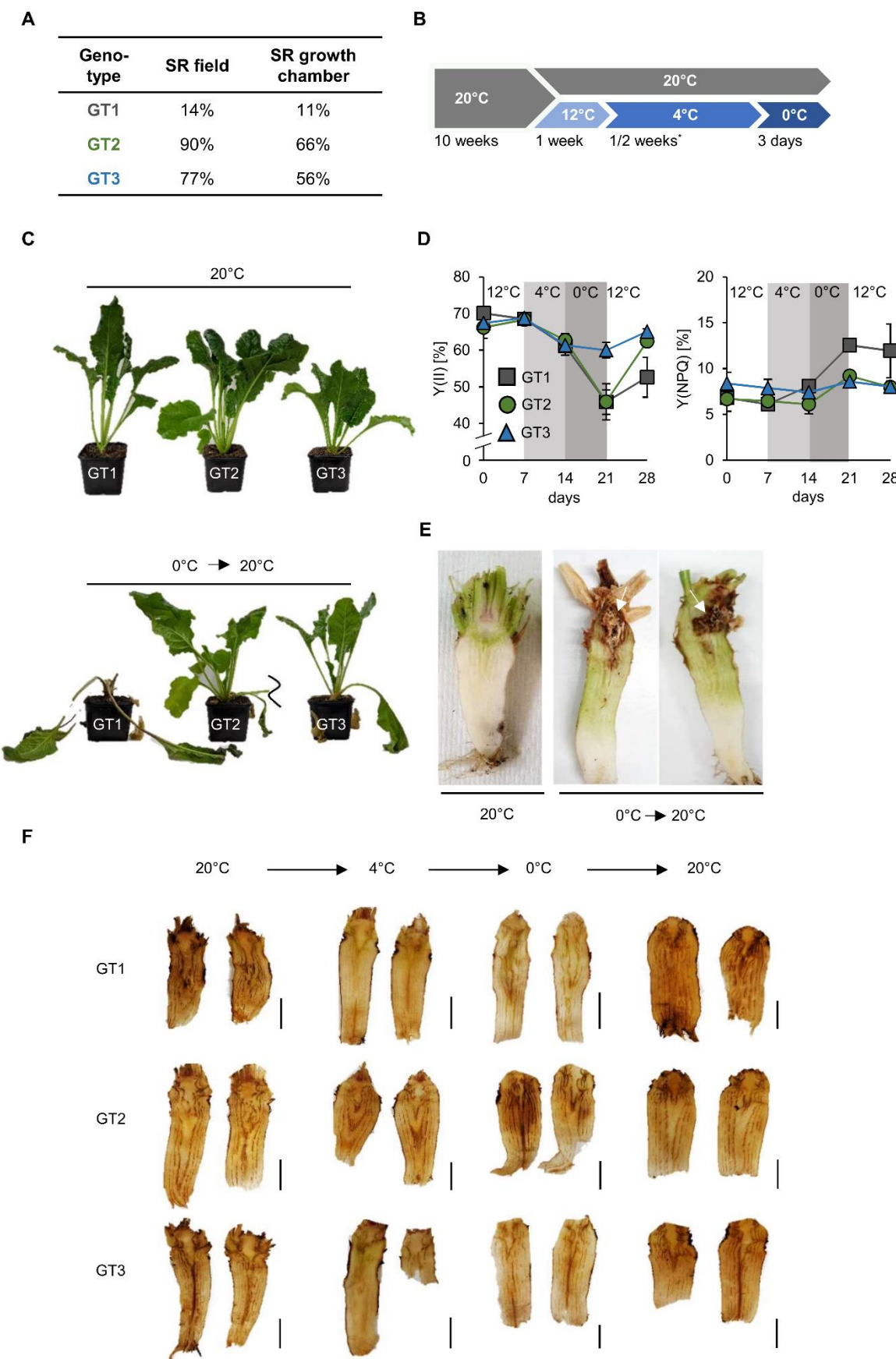

D

E

F

133

8

Figure 1: Responses of sugar beet genotypes to freezing temperatures. (A) Freezing survival rates (SR) of three analyzed sugar beet cultivars GT1, GT2 and GT3 measured under field and growth chamber conditions given in percent of survived plants. (B) Experimental setup for metabolite and photosynthesis measurements. Plants were grown at 20°C for 10 weeks. Subsequently, plants were kept at 20°C(control) or transferred to low temperature acclimation conditions (12°C for one week, and 4°C *one week for photosynthesis measurements, two weeks for RNASeq and metabolite analysis). After 4°C treatment, air temperature in the growth chamber was lowered to -6°C and plants were harvested as soon as the soil temperature was 0°C or below, which was the case three days after transfer to -6°C. (C) Typical appearance of sugar beet plants of GT1, GT2 and GT3 before and after freezing treatment. (D) PAM measurements were performed on leaves of the three different genotypes. For this, air temperature was kept at 0°C. Quantum yield of photosynthesis [Y(II)] and non-photochemical quenching [Y(NPQ)] were measured. Temperature intervals are highlighted in white (12°C), light grey (4°C), or grey (0°C). Values represent the mean of three biological replicates. Error bars represent the standard error of the corresponding mean. Significant changes relative to the control condition (20°C) were calculated independently for each genotype using Student's *t*-test (* $p < 0.05$; ** $p < 0.01$; *** $p < 0.001$). (E) Morphology of sugar beet taproots of genotype GT1 after freezing recovery. Plants were grown at 20°C for 13 weeks and afterwards were shifted to 12°C, 4°C and 0°C and were retransferred to 20°C after freezing treatment. (F) DAB staining indicative for hydrogen peroxide accumulation in longitudinal sections of 10-week old taproots. Scale bars represent 1cm.

The sugar beet taproot is divided into two distinct tissue zones with different sensitivities to freezing

Almost a century ago, plant anatomist Ernst Artschwager noted the anatomic peculiarities of the pith tissue (Artschwager, 1926). Its anatomy differs from other internal taproot tissues, which mainly comprise the storage parenchyma (SP) and vascular tissue (**Fig. 2A**). Our microscopic analysis confirmed Artschwager's observation that the pith consists of spongiform parenchyma cells and revealed that pith cells are more than five times the size of parenchymatic cells alternating with xylem/phloem bundles in the distal parts of the beets (i.e. between the characteristic concentric rings that can be observed in transverse sections, mainly through the below-pith beet tissue) (**Fig. 2B-D**). While the storage parenchyma was drawn with vascular bundles, such long-distance transport tissue was absent from the pith, which was surrounded mostly by primary xylem (**Fig. 2C and 2E**). The

9

164   primary xylem in turn could be traced acropetally towards the vasculature of the oldest leaves and

165   cotyledons, and basipetally to where some of the bundles converge in the central cylinder in below-

166   pith root tissue (**Fig. 2F**). Application of the phloem-mobile carboxyfluoresceine di-acetate (CFDA) to

167   source leaves and subsequent tracking of its green-fluorescent derivative CF in the taproot via

168   confocal microscopy confirmed the occurrence of vascular bundles in storage parenchyma and,

169   importantly, their absence from the pith region (**Fig. 2E and 2F**). To record differential responses in

170   gene expression and metabolite accumulation in SP and pith, we manually separated both tissues.

171   Because of the proximity of the pith to the shoot apical meristem (SAM) **(Fig. 2A)** and with a lack of

172   known markers for the pith, we checked for accumulation of the mRNA of the SAM-marker *CLAVATA2*

173   as indicator for successful enrichment of pith tissue **(Fig. 2G)**. To check whether SP and pith tissue

174   are able to precipitate cold- and freezing treatment under our test conditions, expression of the low

175   temperature response transcription factor *CBF3* was analyzed (**Fig. 2H**). Expression of *CBF3* did not

176   differ between the three analyzed genotypes, but was significantly higher in the pith in comparison

177   to storage parenchyma at 0°C, underlining the marked cold susceptibility of this special tissue (**Fig.**
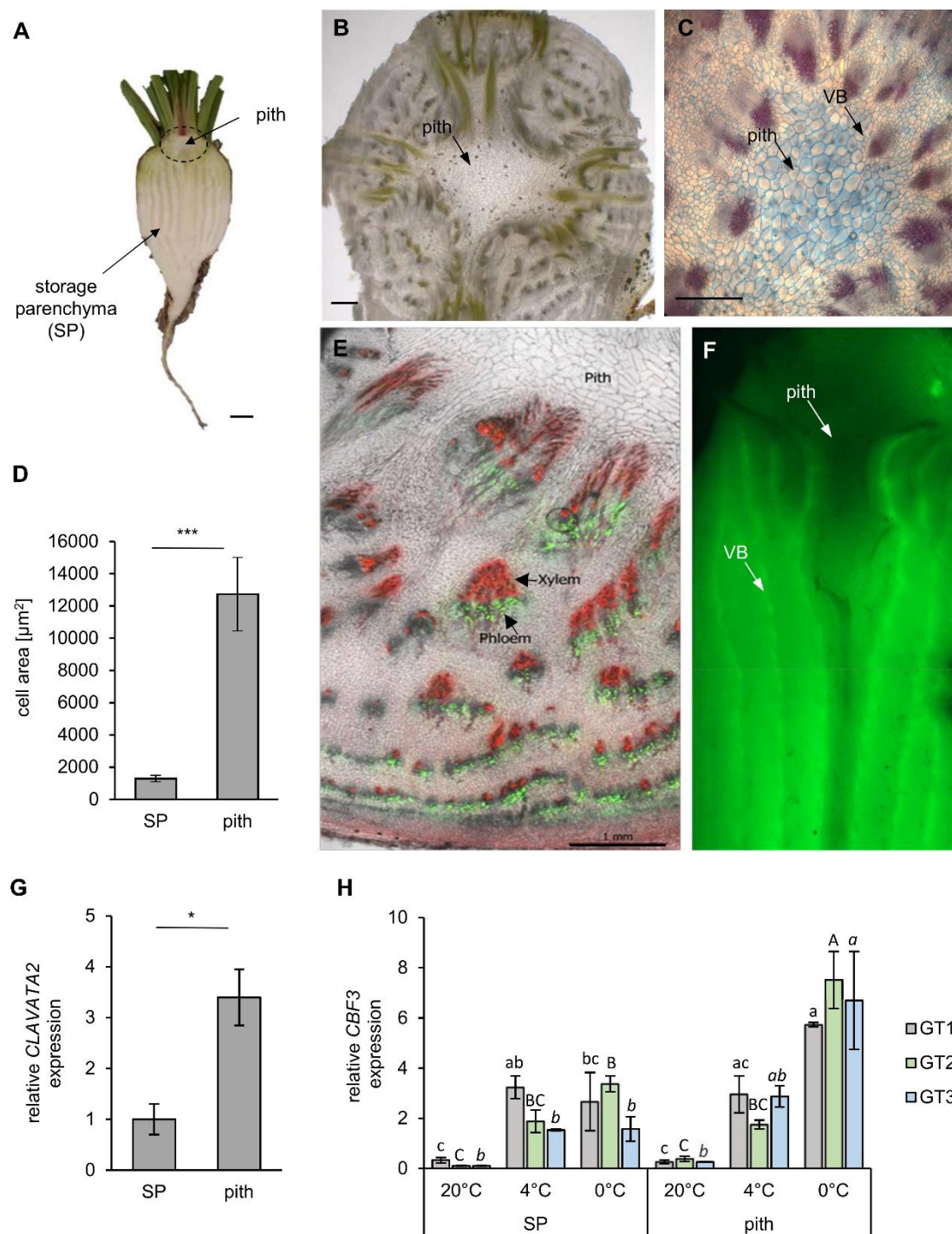
178   **2H**).

179

Figure 2: Morphology of the _B. vulgaris_ pith tissue. (A) longitudinal overview section of a young taproot. Scale bar representing 1cm. (B) Cross section of the pith tissue to reveal its cellular architecture. Scale bar representing 1 mm. (C) FCA staining of a transverse section of the beet hypocotyl including the central pith. Lignified xylem cells are stained in red, while cellulosic cell walls are stained in blue. Scale bar representing 0.5 mm. (D) Mean cell area of storage parenchyma (SP) and pith cells measured in sugar beet cross-sections using
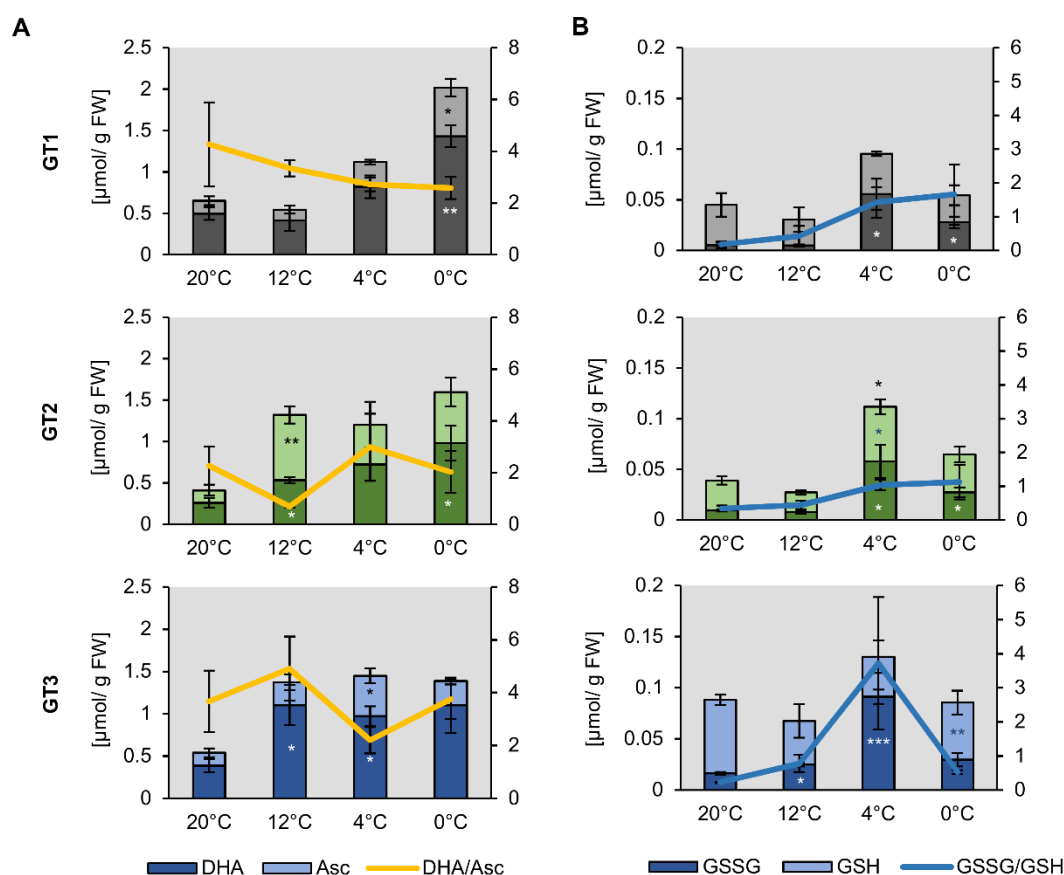
11

185   ImageJ. Error bars represent the standard error over seven cross-sections. (E) Radial phloem-unloading of the

186   fluorescent dye carboxyfluorescein (green). Cell walls were stained with propidium iodine (red), which

187   particularly labels the thick, lignified vessels of the xylem. Scale bar represents 1mm. (F) Carboxyfluorescein

188   unloading and distribution from phloem bundles in the sugar beet taproot. Arrows mark the pith tissue or

189   vascular bundles (VB). (G) Pith and storage parenchyma were separated and expression of the shoot

190   meristematic marker *CLAVATA2 was* analyzed. Error bars represent the standard error over three biological

191   replicates. Asterisks indicate significant differences between pith and storage parenchyma (Student´s *t*-test

192   with * $p<0.05$; *** $p<0.001$ for (D) and (G)). (H) Expression of the cold-induced transcription factor *CBF3* in SP

193   and pith tissue of the three analyzed genotypes. Error bars represent the standard error over three biological

194   replicates. Letters indicate the same level of significance within each of the three genotypes at different temperatures

195   and in different tissues, calculated via two-way ANOVA with post hoc Tukey test with $p< 0.05$.

196

ROS-related genes are upregulated in the taproot pith at low temperatures

198   The prominent staining of ROS in freezing-stressed taproots prompted us to analyze antioxidant

199   levels and expression of ROS-related genes in pith and storage parenchyma of the different sugar beet

200   genotypes (**Fig. 3**). Low temperatures lead to a significant increase of the total ascorbate content (sum

201   of ascorbate and dehydro-ascorbate) but did not significantly alter the ratio of oxidized dehydro-

202   ascorbate to reduced ascorbate in the pith tissues of GT1, GT2 and GT3 (**Fig. 3A**). Glutathione also

203   increased at low temperatures reaching highest levels at 4°C in the pith of all three genotypes. The

204   ratio of oxidized GSSG to reduced GSH, serving as an indicator for the ROS stress-level of the tissue,

205   strongly increased with decreasing temperature, reaching its highest value at 0°C in GT1 and GT2, or

206   at 4°C in GT3 (**Fig. 3B**). Compared to the antioxidant contents in the pith, the contents in the storage

207   parenchyma developed similarly with decreasing temperature, but the glutathione contents in the

208   storage parenchyma were overall lower compared to the pith tissue of the different sugar beets

209   (**Supplemental Fig. S1B**). Together with levels of antioxidants, gene expression was monitored in

210   pith and SP tissue during cold- and freezing exposure (**Fig. 3C**). Tissues were analyzed under control

211   temperature (20°C), after one week at 4°C, or after an additional three days at 0°C. Most of the tested

212   genes were upregulated in plants subjected to low temperature treatment, but the increase in

213   expression was always stronger in the pith compared to the SP. Genes encoding typical ROS-

214   scavenging enzymes like catalase, ascorbate peroxidase and reductase, as well as glutathione

215   peroxidase showed the highest expression at 4°C and tuned down again at 0°C. Interestingly,

216   expression of homologs to H_2O_2- and superoxide-responsive transcription factor genes *ZAT10* and

217   *ZAT12* increased markedly at 0°C, but not at 4°C (**Fig. 3A**) with highest upregulation observed in the

218   pith tissue, indicating that ROS accumulation increased at 0°C and suggesting that ROS detoxification

219   efficiency was lower at 0°C in comparison to 4°C.

220   In summary, these results indicate that low temperature-dependent ROS formation and response to

221   ROS accumulation was most pronounced in the pith area of taproots and support the higher

222   accumulation of ROS revealed by ROS staining (**Fig. 1F**).

223

A

GT1, GT2, GT3 — y-axis [µmol/ g FW]; x-axis 20°C, 12°C, 4°C, 0°C

B

GT1, GT2, GT3 — y-axis [µmol/ g FW]; x-axis 20°C, 12°C, 4°C, 0°C

Legend (A): ■ DHA ■ Asc ― DHA/Asc
Legend (B): ■ GSSG ■ GSH ― GSSG/GSH

C

enzyme	reaction	gene symbol	homology (*A.t.*)	gene locus (*B.v.*)	GT	Pith 20°C	Pith 4°C	Pith 0°C	SP 20°C	SP 4°C	SP 0°C
transcription factors	H_2O_2 response	*ZAT10*	*AT1G27730*	*BVRB_8g189640*	GT1	ns	ns	ns	ns	ns	ns
					GT2	b	b	a	b	b	ab
					GT3	b	b	a	b	b	b
	superoxide response	*ZAT12*	*AT5G59820*	*BVRB_2g037310*	GT1	bc	bc	a	c	ac	ab
					GT2	b	ab	a	b	ab	ab
					GT3	b	b	a	b	b	b
Superoxide-dismutase	$2O_2^- + 2H^+ \rightarrow H_2O_2 + O_2$	*SOD*	*AT2G28190*	*BVRB_9g206190*	GT1	ns	ns	ns	ns	ns	ns
					GT2	ns	ns	ns	ns	ns	ns
					GT3	ab	a	ab	b	ab	b
Catalase	$2H_2O_2 \rightarrow 2H_2O + O_2$	*CAT*	*AT1G20630*	*BVRB_1g021080*	GT1	b	a	b	b	a	b
					GT2	c	a	c	bc	ab	bc
					GT3	bc	ab	ac	c	a	c
Ascorbate peroxidase	$2Asc + H_2O_2 \rightarrow 2MDA + 2H_2O$	*APX*	*AT1G07890*	*BVRB_9g207350*	GT1	bc	a	bc	bc	ab	c
					GT2	ab	a	b	ab	ab	b
					GT3	ab	a	bc	ab	ab	c
Monodehydro-ascorbate reductase	$MDA + NAD(P)H+H^+ \rightarrow Asc + NAD(P)^-$	*MDAR*	*AT3G52880*	*BVRB_7g159920*	GT1	bc	a	ab	bc	ac	c
					GT2	c	a	c	c	b	c
					GT3	cd	a	bc	cd	ab	d
Dehydro-ascorbate reductase	$DHA + 2GSH \rightarrow Asc + GSSH$	*DHAR*	*AT5G16710*	*BVRB_2g039390*	GT1	bc	a	bc	bc	ab	c
					GT2	b	a	bc	bc	bc	c
					GT3	a	a	ab	ab	a	b
Glutathione peroxidase	$H_2O_2 + 2GSH \rightarrow 2H_2O + GSSG$	*GPX*	*AT4G31870*	*BVRB_2g044150*	GT1	ab	a	ab	ab	ab	b
					GT2	b	a	b	bc	bc	c
					GT3	ab	ab	a	b	ab	b
Glutathione reductase	$GSSG + NAD(P)H \rightarrow 3GSH + NAD(P)^-$	*GR*	*AT3G24170*	*BVRB_3g069540*	GT1	b	ab	ab	b	a	ab
					GT2	c	c	a	c	c	b
					GT3	b	a	b	b	b	b

224

14

225 **Figure 3: ROS related metabolite accumulation and gene expression.** (A) and (B) Concentrations of
226 ascorbate (Asc) and dehydro-ascorbate (DHA) (A) or reduced (GSH) and oxidized glutathione (GSSG) (B) in the
227 pith of different sugar beet genotypes. Reduced form of the antioxidant depicted in light, oxidized form in dark
228 color. Sugar beet plants were grown for 10 weeks at 20°C and were successively transferred to 12°C, 4°C and
229 0°C for one week each. Three plants of each genotype were harvested at a given temperature and were analyzed
230 for their antioxidant concentration. Error bars represent the standard error over the corresponding mean.
231 Asterisks indicate significant differences in concentrations of reduced, or of oxidized antioxidants or of the
232 oxidized/ reduced ratio calculated in relation to the corresponding values at 20°C using Student´s t-test (* p<
233 0,05; ** p< 0.01). (C) Heat map representation of RT-qPCR analysis of ROS relates genes in taproot pith and
234 storage parenchyma (root) from the three genotypes grown at control (20°C) or low temperatures (4°C and
235 0°C). Data represents the mean of three independent biological replicates. Different letters within individual
236 tiles denote significant differences between tested conditions and tissues according to two-way ANOVA with
237 post-hoc Tukey HSD testing (p<0.05).

238

The pith tissue is metabolically separated from taproot parenchyma and altered after exposure to subzero temperatures
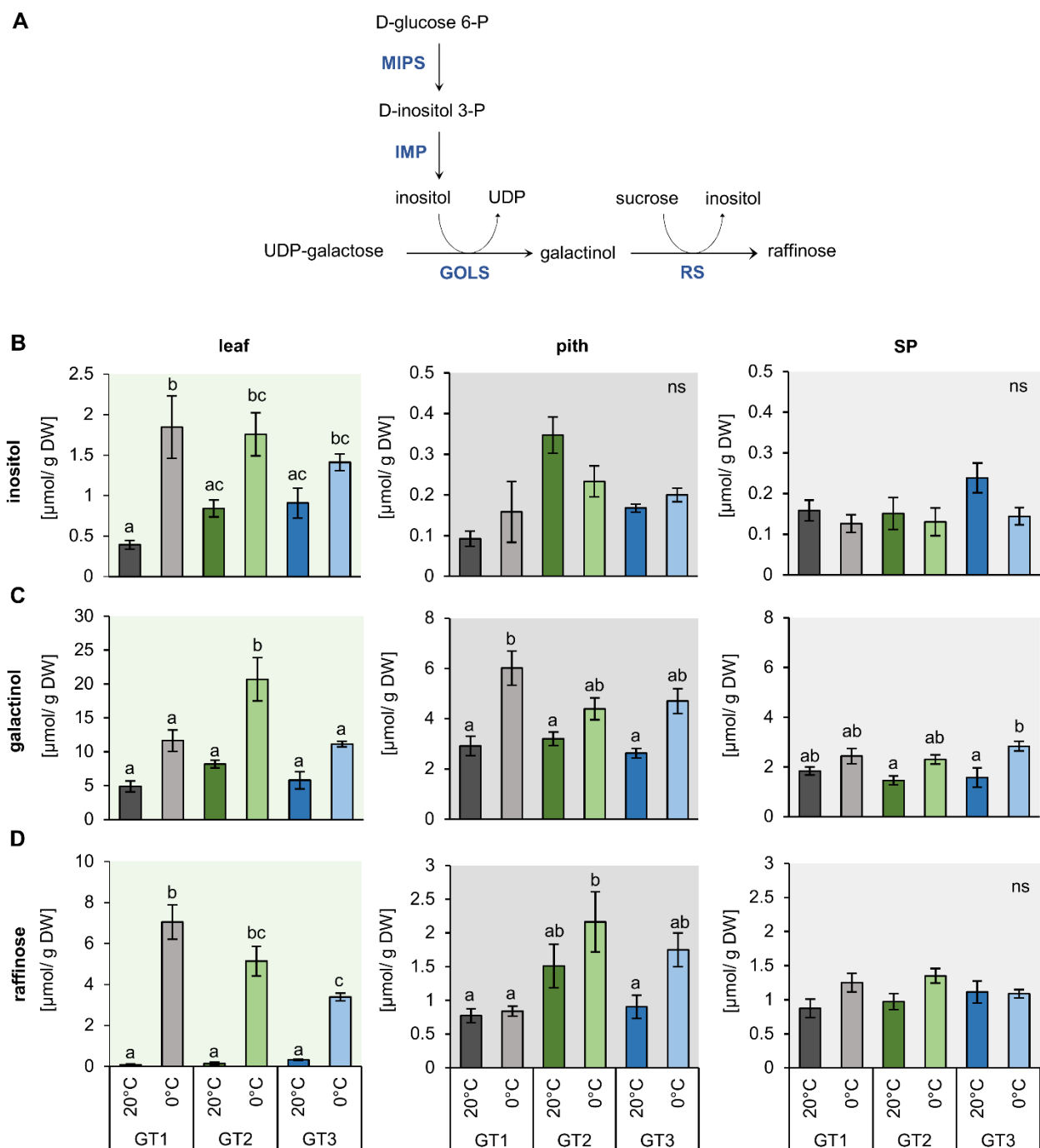
241 In addition to the antioxidants ascorbate and glutathione, also other compounds like sugars and

242 amino acids contribute to ROS scavenging. Since ROS accumulation was pronounced in the pith region

243 of taproots, we analyzed the low temperature-dependent accumulation of such metabolites and their

244 spatial distribution between leaf, pith, and storage parenchyma tissues. In total, 36 compounds were

245 measured and their contents are listed in **Supplemental Table S1**. A PC analysis, loaded with the

246 0°C/20°C fold-changes of these compounds PC1 separated pith and SP tissues (**Supplemental Figure**

247 **S2**). The metabolic reaction of the storage parenchyma of the two more tolerant genotypes, GT2 and

248 GT3, was similar, but differed from that of GT1 (**Supplemental Figure S2**). The separation of leaf

249 tissue from pith and storage parenchyma was mainly based on changes in raffinose concentrations

250 (**Supplemental Figure S2**). Different degrees of changes in starch content mainly contributed to the

251 separation of pith and storage tissue (**Supplemental Figure S2**). Under control temperatures, the

252 starch content of leaves exceeded that of pith and storage parenchyma about 10-fold (**Supplemental**

253 **Figure S3**). After exposure to frost, starch decreased drastically in leaves, but was not significantly

15

254   altered in pith and storage parenchyma (**Supplemental Figure S3**). However, only low

255   concentrations of starch are present in the sugar beet taproot tissue in general and therefore starch

256   is unlikely to contribute significantly to frost-tolerance (Rodrigues et al., 2020; Turesson et al., 2014).

257   Changes in starch content, however, depend on soluble sugar metabolism. Consistently, frost also

258   massively increased concentrations of glucose and fructose in leaves, but not significantly in pith and

259   storage tissues (**Supplemental Figure S3**). Sucrose concentrations were highest in the storage

260   parenchyma and lowest in the leaves (**Supplemental Figure S3**). In both tissues no significant

261   changes in sucrose concentrations could be observed between control and freezing conditions, or

262   between genotypes (**Supplemental Figure S3**). In the pith tissue, concentrations of sucrose differed

263   at 20°C between genotypes, but fluctuated only marginally within and between genotypes at 0°C

264   (**Supplemental Figure S3**).

265   **Genotype and temperature-dependent accumulation of inositol, galactinol, and raffinose**

266   As concentrations of glucose, fructose and sucrose differed only marginally in pith tissues of the three

267   genotypes after a shift from control to freezing conditions, we analyzed the contents of raffinose as

268   well as of inositol and galactinol, which are precursors for raffinose synthesis (**Fig. 4A**), because

269   raffinose was shown to possess second order rate constants for ROS scavenging, comparable or even

270   higher than those of glucose, fructose and sucrose and the antioxidant ascorbate (Nishizawa et al.,

271   2008). Similar to the sugars glucose, fructose, and sucrose, the pith tissue had inositol, galactinol and

272   raffinose concentrations in-between of those measured for leaves and taproot SP (**Fig. 4**). Inositol

273   content of the leaves at 20°C was highest in GT2 and GT3. Upon 0°C exposure, inositol levels increased

274   to comparable amounts in the leaf tissue of all three genotypes (**Fig. 4B**). However, in the pith and

275   storage parenchyma, inositol levels remained unchanged upon exposure to freezing temperatures

276   (**Fig. 4B**). Like its precursor inositol (**Fig. 4A**), concentrations of galactinol increased in leaves at 0°C

277   two- to three-fold **(Fig. 4C)**. Galactinol concentrations also increased in the pith and storage tissue at

16

278   0°C. In the pith galactinol accumulated at 0°C to concentrations twice as high as compared to the SP

279   (**Fig. 4C**). Notably, freezing temperatures boosted raffinose concentrations at least 10-fold, in GT3

280   leaves, and up to 80-fold, in GT1 leaves, in comparison to the corresponding leaf-tissue at 20°C (**Fig.**

281   **4D**). In the pith tissue, raffinose content increased in GT2 and GT3 at 0°C. At 0°C, raffinose levels of

282   GT2 and GT3 exceeded those of GT1 at least two-fold in the pith. Interestingly, GT2, the cultivar with

283   the highest freezing survival rates (**Fig. 1A**), had about 80% higher raffinose concentrations in

284   comparison to GT1 and GT3 already under control conditions (**Fig. 4D**). In SP, raffinose

285   concentrations were slightly increased or remained unchanged at 0°C in comparison to 20°C (**Fig.**

286   **4D**).

Figure 4: Inositol and raffinose synthesis and their concentrations in leaf, pith and storage parenchyma tissue under control and freezing temperatures. (A) Schematic representation of inositol and raffinose synthesis in plants. (B) to (D) Raffinose and intermediates in raffinose synthesis were measured in plants grown at 20°C and plants transferred to 12°C, 4°C and harvested at 0°C soil temperature. Plants were dissected in the three different tissues leaf, pith and root while harvesting at the corresponding temperatures. Inositol (B), galactinol (C) and raffinose (D) concentrations represent the mean of three biological replications for each of the tested cultivars. Error bars represent

18

294   the standard error over the corresponding mean. Letters indicate the same level of significance for each measured

295   concentration, calculated via two-way ANOVA with post hoc Bonferroni test with $p < 0.05$.

296

297   **Inositol-, galactinol- and raffinose-biosynthesis genes are differentially expressed in leaf and**

298   **taproot tissue in response to freezing**

299   To reveal global patterns of gene expression in response to freezing stress we performed comparative

300   RNASeq analysis of leaf and taproot tissues of the three different genotypes at control and freezing

301   temperatures. However, this analysis came with the limitation that we did not separate pith and

302   storage parenchyma but instead analyzed total taproots. RNA-Seq reads were mapped to the sugar

303   beet reference genome (Dohm et al., 2013) and revealed global rearrangement of gene expression in

304   leaf and taproot tissue upon freezing exposure (**Fig. 5A, B and Fig. 5F, G**).

305   To get a more general overview on regulation of different cellular pathways and reactions, RNASeq

306   data were mapped into different functional groups, based on MapMan mapping. We then calculated

307   the mean logarithmic fold change (log2FC) of all genes with log2FC ≠ 0 mapped in each of these

308   functional groups, without filtering for significant changes prior to analysis. This analysis revealed

309   downregulation of genes involved in photosynthesis in leaf tissue at 0°C (**Fig. 5C**). In contrast, minor

310   CHO metabolism was the most prominently upregulated functional group in the leaf (**Fig. 5C**) and

311   also in the taproot tissue (**Fig 5H**). Minor CHO metabolism separates into the sub-bins raffinose,

312   inositol, sugar alcohols, galactose, trehalose, callose synthesis, and sugar kinases. The mean log2FCs

313   of genes involved in each of these sub-bins ranged from lowest values for sugar alcohols to highest

314   for raffinose metabolism in leaves and from lowest mean log2FC for inositol to highest for raffinose

315   metabolism in taproot tissue (**Fig. 5D and 5H**). The latter opposite regulation of inositol and raffinose

316   in taproots is interesting because inositol is essential for raffinose biosynthesis and the high log2FCs

317   for raffinose in both leaves and taproots suggested increased utilization of carbon for raffinose

19

318   biosynthesis under low temperatures. To reveal first genotype dependent differences in the

319   expression of minor CHO genes in the different genotypes, violin plots showed the distribution of

320   log2FC over minor CHO genes in leaf and taproot tissues. While most of those genes show log2FCs

321   between -2 and 2 in both leaf and taproot tissues upon freezing treatment (**Fig. 5E and 5J**), in GT2 a

322   few genes showed log2FC of up to 7 in the leaves and up to 10 in the taproot (**Fig. 5E and 5J**). Overall

323   the number of highly upregulated genes in minor CHO metabolism of GT2 was higher than in GT1 and

324   GT3, independent of the tissue (**Fig. 5E and 5J**). To reveal possible genotype specific regulation of

325   genes involved in raffinose and its precursors synthesis, we extracted transcript levels for those genes

326   upon exposure to 0°C (**Table 1**).
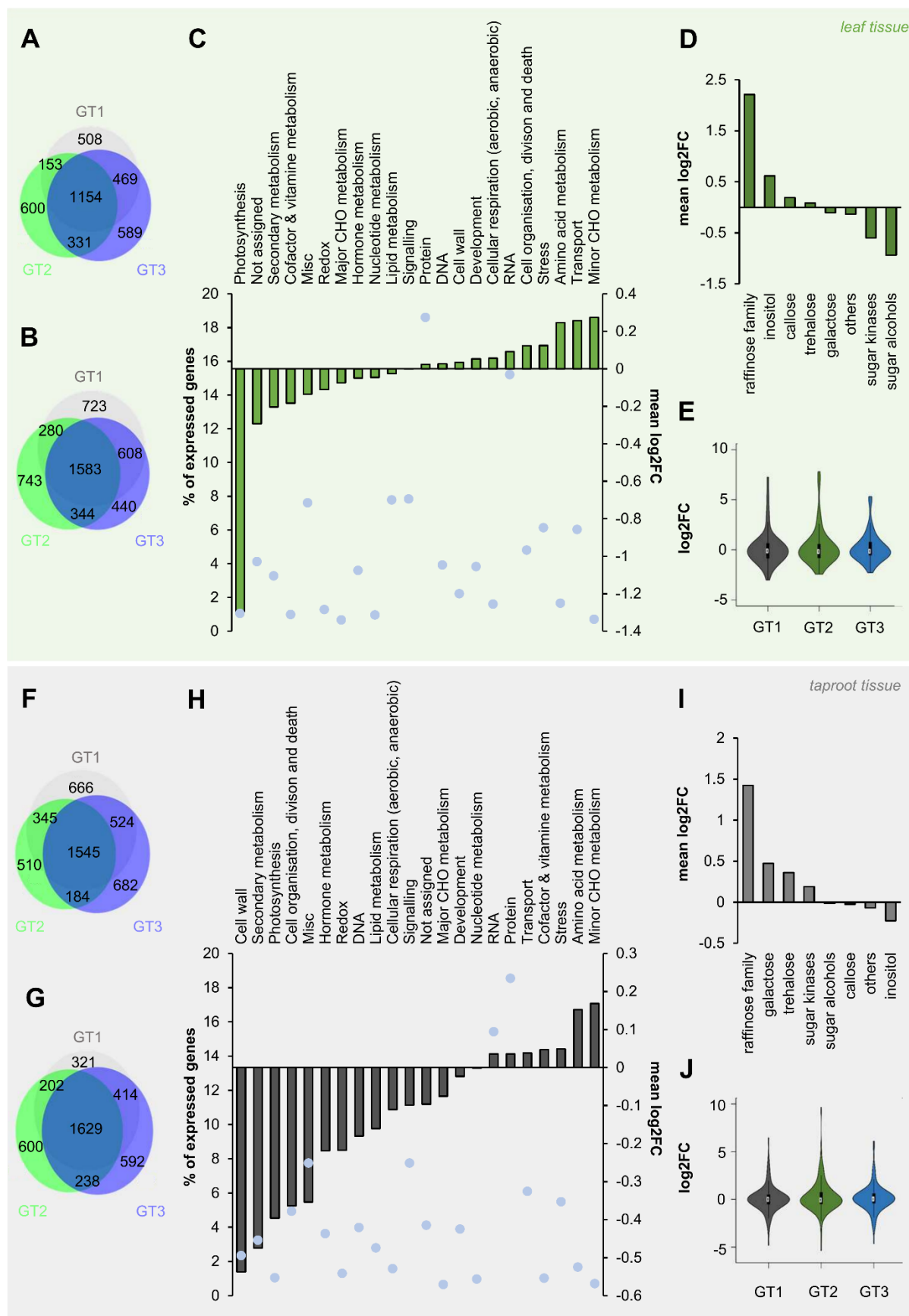
327

329 **Figure 5: Changes in gene expression of *B. vulgaris* leaf and taproot tissues upon freezing treatment.** (A,
330 b; F, G) Venn diagrams of differentially expressed genes in leaves (A, B) and taproots (F, G). Numbers of up –
331 (Log2FC ≥ 1; A, F) or down – (Log2FC ≤ -1; B, G) regulated genes (with a FDR ≤ 0.05) in leaves (A, B) or taproots
332 (F, G) are given inside the circles of the diagram. Log2FC 20°C/ 0°C of all expressed genes with log2FC ≠ 0 in
333 leaf (C) and taproot tissue (H) were functionally grouped and plotted against the number of genes in each group
334 given in percent of the total number of expressed genes (blue dots). (D) and (I) mean $\log_2$FC 20°C/ 0°C of genes
335 with log2FC ≠ 0 of different metabolic pathways included in the functional group of "minor CHO metabolism"
336 in leaf (D) and taproot tissue (I). Log2FCs represent the mean of the three different *B. vulgaris* genotypes GT1,
337 GT2 and GT3, each measured in three biological replications for (C, D) in the leaf and (H, I) in the taproot.
338 Log2FCs of genes included in the functional group of "minor CHO metabolism" are shown as violin plots for the
339 corresponding tissues leaf (E) and taproot (J). White circles show the medians, box limits indicate the 25th and
340 75th percentiles as determined by R software, whiskers extend 1.5 times the interquartile range from the 25th
341 and 75th percentiles and polygons represent density estimates of data and extend to extreme values in violin
342 plots.

343 **Table 1: Log2FC 20°C/ 0°C of expression of enzymes involved in inositol-, galactinol and raffinose**
344 **synthesis of leaf and taproot tissue** (root) of three differential *B. vulgaris* genotypes GT1, GT2 and GT3. Data
345 have been extracted from the RNASeq analyis. Significant up- or downregulation at 0°C in comparison to the
346 expression at 20°C is indicted by bold numbers. Significance was calculated using Student´s *t*-test with false
347 discovery rate testing (p_{adj} <0.1).

Function	Gene identifier (RefBeet1.2)	Gene name	Annotation	leaf GT1	leaf GT2	leaf GT3	root GT1	root GT2	root GT3
inositol biosynthesis	Bv6_135490_ioyj.t1	MIPS	inositol-3-phosphate synthase (*M. crystallinum*)	3.46	**3.68**	3.17	0.96	**1.85**	0.49
	Bv3_059200_pzry.t1	IMP1	type I inositol polyphosphate 5-phosphatase (*A. thaliana*)	-1.89	-1.02	-0.96	-3.27	-2.49	-3.04
	Bv4_097150_xtnp.t1	IMP2	bifunctional phosphatase IMPL2, precursor (*A. thaliana*)	0.60	0.32	0.91	0.89	0.58	0.65
	Bv5_127150_wkgm.t1	IMP3	phosphatase IMPL1, precursor (*A. thaliana*)	-1.19	-1.27	-1.08	-0.01	-0.01	0.20
	Bv8_184830_ufws.t1	IMP4	inositol monophosphatase (*M. crystallinum*)	0.22	0.31	0.71	-0.56	-0.50	-0.64
	Bv9_217040_nmtf.t1	IMP5	bifunctional phosphatase IMPL2, precursor (*A. thaliana*)	-0.27	-0.21	-0.40	-0.46	-0.55	-0.81
galactinol biosynthesis	Bv5_122490_gtzu.t1	GOLS1	galactinol synthase 1 (*A. thaliana*)	**7.18**	7.57	5.33	**2.33**	**1.79**	2.24
	Bv4_079980_rfmk.t1	GOLS2	galactinol synthase 2 (*S. lycopersicum*)	5.65	**7.06**	5.01	0.55	**2.97**	1.14
	Bv4_080000_ugrr.t1	GOLS3	galactinol synthase 2 (*S. lycopersicum*)	7.25	7.81	5.26	6.46	**9.88**	6.11
	Bv6_155630_dgxc.t1	GOLS4	galacturonosyltransferase-like (*A. thaliana*)	-3.00	-2.43	-1.42	-4.82	**-5.37**	-4.64

22

raffinose biosynthesis	Bv4_091140_xstd.t1	RS1	galactinol-sucrose galactosyltransferase 1 (*A. thaliana*)	-2.94	-2.30	-2.28	-2.22	-1.57	-2.39
	Bv_006460_trdy.t1	RS2	galactinol-sucrose galactosyltransferase 2 (*A. thaliana*)	0.86	0.78	0.91	2.09	**1.95**	1.82
	Bv7_177120_psfp.t1	RS3	galactinol-sucrose galactosyltransferase 2 (*A. thaliana*)	0.55	0.54	0.33	-0.09	-0.29	-0.13
	Bv1_011340_dsoj.t1	RS5	galactinol-sucrose galactosyltransferase (*P. sativum*)	**4.51**	**6.26**	4.77	3.33	**3.36**	**2.89**
	Bv8_193750_qhjs.t1	RS6	galactinol-sucrose galactosyltransferase 6 (*A. thaliana*)	-0.19	-0.45	-0.15	0.31	0.50	-0.33

348

349 *De-novo* inositol biosynthesis occurs via the enzymes myo-inositol phosphate synthase (MIPS) and

350 inositol monophosphatase (IMP) (**Fig. 4A**; Loewus and Murthy, 2000). MIPS catalyzes the rate

351 limiting step in inositol *de-novo* synthesis (Donahue et al., 2010), isomerization of glucose-6-

352 phosphate to inositol-3-phosphate. IMP then catalyzes de-phosphorylation of inositol-3-phosphate to

353 inositol. In the *B. vulgaris* genome (Dohm et al., 2013), we identified one sequence with high homology

354 to MIPS (*Bv*MIPS, Bv6_135490_ioyj.t1) and five sequences with high homology to IMP (*Bv*IMP1,

355 Bv3_059200_pzry.t1; *Bv*IMP2, Bv4_097150_xtnp.t1; *Bv*IMP3, Bv5_127150_wkgm.t1; *Bv*IMP4,

356 Bv8_184830_ufws.t1; *Bv*IMP5, Bv9_217040_nmtf.t1).

357 Frost enhanced expression of *BvMIPS* in both, leaves and taproots, with the strongest induction

358 occurring in the freezing-tolerant cultivar, GT2 (**Table 1**). Expression of the five *IMP* genes was

359 differentially regulated upon 0°C. In leaves, *IMP1*, *IMP3*, and *IMP5* were downregulated, while *IMP2*

360 and *IMP4* genes were slightly upregulated at 0°C. In taproots, IMP expression was downregulated,

361 except for IMP2 (**Table 1**). However, *IMP* genes were not regulated in a genotype-dependent manner.

362

363   Inositol can be fused to UDP-galactose to form alpha-D-galactosyl-(1->3)-1D-myo-inositol

364   (galactinol) and UDP. This reaction is catalyzed by galactinol synthase (GOLS) and is required for

365   subsequent biosynthesis of raffinose (**Fig. 4A**). We identified four genes with homology to galactinol

366   synthases from tomato (*Solanum lycopersicum*) or Arabidopsis in the sugar beet genome (**Table 1,**

367   **Supplemental Figure S4**). The expression of three of the four *GOLSs* (*BvGOLS1 to 3*) was strongly

368   upregulated at 0°C in leaves and in taproots. The log2FCs for *GOLS2* and *GOLS3* in leaves and

369   especially in the taproot of GT2 exceeded those of the less freezing tolerant genotypes GT1 and GT3

370   (**Table 1**). The gene coding for a fourth GOLS isoform, *GOLS4*, was downregulated at 0°C, independent

371   of the tissue and genotype (**Table 1**). Phylogenetic analysis revealed that *BvGOLS4*

372   (Bv6_155630_dgxc.t1) was only distantly related to the other sugar beet GOLS isoforms

373   (**Supplemental Figure S4**) and therefore may not encode a functional GOLS or a GOLS relevant for

374   the plants freezing response.

375

376   The ultimate step of raffinose biosynthesis is the transfer of the galactinol's galactose moiety to

377   sucrose via the enzyme raffinose synthase (RS). During this reaction, inositol is released from

378   galactinol (**Fig. 4A**). We identified seven RS isoforms in the sugar beet genome (**Supplemental Figure**

379   **S4**). Two isoforms, *BvRS4* and *BvRS7* were not changed in their expression. Of the remaining 5

380   isoforms, two RS, *BvRS2* and *BvRS5*, were upregulated in the leaf and taproot tissue at 0°C (**Table 1**).

381   Overall, *BvRS5* (*Bv1_011340_dsoj.t1*), the closest homolog to *AtRS5* (**Supplemental Figure S4**),

382   showed the highest upregulation at 0°C (**Table 1**). Similar to the GOLS genes, upregulation was

383   strongest in freezing-tolerant GT2 plants, independent of the tissue (**Table 1**).

384

385

386

24

387 **Raffinose biosynthesis genes are induced in pith tissues at low temperatures in a genotype-**

388 **dependent manner**

389 The RNAseq analysis suggested that raffinose metabolism is important in both leaf and taproot tissues

390 during the freezing response of sugar beet plants (**Figure 5 and Table 1**). Because of the different

391 sensitivities of the pith of the three genotypes to freezing, we analyzed the expression of galactinol

392 and raffinose biosynthesis-related genes in taproot tissues with RT-qPCR (**Fig. 6**). Among galactinol

393 synthases, *GOLS1* was the most abundant isoform in the pith and storage parenchyma (**Fig. 6A**),

394 however, upregulation of gene expression in terms of fold-change was strongest for *GOLS2* and *GOLS3*

395 at 0°C (**Fig. 6A**). Expression of *GOLS2* and *GOLS3* was highest in GT1 and GT3 at 0°C (**Fig. 6A**). The

396 two RS isoforms *RS2* and *RS5* showed comparable abundance in the pith of all three genotypes at

397 control temperatures. Abundance of *RS2* was slightly higher in the storage parenchyma, while *RS5*

398 abundancy in the SP was comparable to the pith at 20°C (**Fig. 6B**). Additionally, the upregulation of

399 RS expressions in terms of fold- change in the pith was comparable between *RS2* and *RS5* expression

400 in GT2 and GT3. Overall, GT3 showed the highest fold-change upregulation of *RS2* and *RS5* in the pith

401 (**Fig. 6B**). In GT1 pith tissue, upregulation of *RS2* expression was comparable to that in GT2 (**Fig. 6B**).

402 While *RS2* was upregulated in the pith of GT1 upon exposure to 0°C, GT1 pith tissue lacked the ability

403 of upregulation of *RS5* upon exposure to freezing temperatures (**Fig. 6B**). While *RS5* expression

404 increased more than 15-, and 20- fold in the pith of GT2 and GT3 respectively, expression remained

405 unaltered in the pith of the less tolerant GT1 upon 0°C (**Fig. 6B**). GT1 failed to induce *RS5* in the pith

406 tissue in comparison to GT2 and GT3 and induction of *RS5* expression was highest in SP of this

407 genotype (**Fig. 6B**). Taken together, expression of *RS* genes in the pith was upregulated to a greater

408 extent in the freezing-tolerant cultivars GT2 and GT3, and to a lower extent in sensitive GT1 (**Fig. 6B**),

409 which is in line with the low raffinose concentrations in the pith of this genotype at 0°C (**Fig. 4D**).
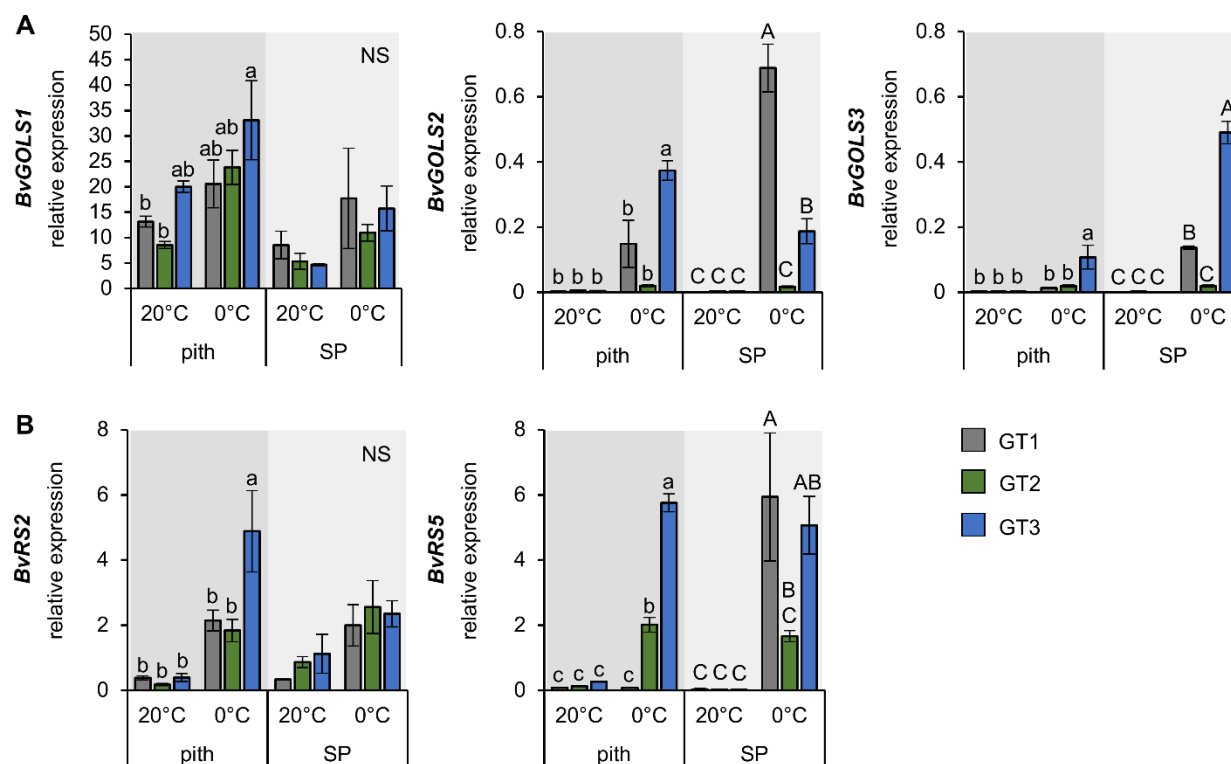
Figure 6: Expression of *GOLS* and *RS* isoforms in pith and storage parenchyma samples of three contrasting *B. vulgaris* cultivars. Relative expression of *GOLS* (A) and *RS* isoforms (B) in the pith and storage parenchyma at 20°C and freezing treatment at 0°C. Bars represent means from three biological replicates ± standard error. Different letters indicate significant differences between genotypes within a tissue according to two-way ANOVA with post hoc Tukey test ($p < 0.05$).

DISCUSSION

During exposure to low temperatures (4°C), sugar beet plants undergo a transformation in metabolite- and gene expression profiles (Rodrigues et al., 2020). However, as we show here, not only chilling but also freezing treatment induces changes in metabolite concentrations and gene expression. Because *Beta vulgaris* is a freezing-sensitive plant showing severe freezing-induced tissue damage (**Fig. 1C**), it is of high interest to analyze the plant's response to sub-zero temperatures on a molecular basis.

424   Transcriptomic analysis revealed that genes involved in minor CHO metabolism were strongly

425   upregulated in both leaf- and taproot tissues (**Fig. 5 and Table 1**). While genes from this functional

426   group were upregulated, genes involved in photosynthesis were downregulated upon freezing

427   treatment (**Fig. 5**). Both the downregulation of photosynthesis-related genes and the decrease in

428   photosynthetic activity (**Fig. 1D**) at low temperatures confirmed our recent results, where cold (4°C)

429   treatment led to lower photosynthetic activity and downregulation of photosynthesis-genes in sugar

430   beet leaves (Rodrigues et al., 2020). Such effects on photosynthetic related protein level has also been

431   observed in leaves of Arabidopsis (Fanucchi et al., 2012; Janmohammadi et al., 2015) and may be a

432   direct effect of electron overflow at photosynthetic reaction centers because of a slow-down of Calvin-

433   Benson cycle reactions (Pommerrenig et al., 2018; Strand et al., 1997).

434   Sugar concentrations, especially those of monosaccharides, increased at 0°C in the leaf tissue

435   (**Supplemental Figure S3**) in a similar manner as in other plant species, where metabolites

436   accumulate during prolonged cold treatment (Ho et al., 2020; Klemens et al., 2014; Usadel et al.,

437   2008). Overall, concentrations of sucrose were highest in the heterotrophic tissues, whereas

438   concentrations of the monosaccharides glucose and fructose were highest in the leaves

439   (**Supplemental Figure S3**). This pattern was expected, as sucrose is the main storage carbohydrate

440   of taproots (Giaquinta, 1979; Rodrigues et al., 2021). The pith tissue harbored intermediate

441   concentrations of both, monosaccharides and sucrose, as - in contrast to the storage parenchyma – it

442   is not directly supplied with sucrose by the phloem. The application of the phloem mobile stain CFDA

443   (Knoblauch et al., 2015; Mehdi et al., 2019; Pommerrenig et al., 2020) to source leaves allowed

444   visualization of phloem fluxes into and within the sugar beet taproot and indicated that sucrose was

445   transported in the taproot via the phloem in a similar manner. CFDA staining revealed organization

446   of the phloem in vascular rings surrounding the pith (**Fig. 2**). Sugar translocated via and unloaded

447   from the phloem can therefore not directly enter the pith tissue (**Fig. 2**) (Artschwager, 1926; Jahnke

448   et al., 2009; Metzner et al., 2014). This observation correlates with lower amounts of sucrose in the

449   pith tissue (**Supplemental Figure S3**). The size of pith cells was markedly larger in comparison to

450   storage parenchyma cells and morphology of the pith already suggests lower sucrose concentrations

451   in its cells, since sucrose concentration has been reported to decline with cell size in sugar beet (Bellin

452   et al., 2007).

453   Our observations show that post-freezing rot of taproot tissue mainly originates from the pith tissue.

454   High ROS accumulation at freezing temperatures as indicted by intense DAB- and NBT-derived

455   staining (**Fig. 1 and Supplementary Figure S1**) and strong upregulation of ROS marker genes *ZAT10*

456   and *ZAT12* (**Fig. 3**) might be causative for the observed tissue damage resulting in post-freezing

457   rotting of the pith. Genes encoding factors of the ROS detoxification system were markedly

458   upregulated at chilling temperatures (4°) or freezing temperatures (**Fig. 3**). Raffinose biosynthesis

459   genes on the other hand were also increased at 4°C but maintained high mRNA levels at 0°C (**Fig, 5**

460   **and Table 1**).

461   Raffinose is known to accumulate under abiotic stress conditions such as drought (Li et al., 2020) or

462   cold in different plant species including Arabidopsis and rice (*Oryza sativa*) (Saito and Yoshida, 2011;

463   Taji et al., 2002). Raffinose is synthesized by a transfer reaction of galactosyl units to sucrose,

464   involving the enzymes galactinol synthase (GOLS) and raffinose synthase (RS) (**Fig. 4A**). Both

465   enzymes were reported to be upregulated during cold treatment in *Ajuga reptans, Medicago falcata,*

466   *Medicago sativa* or *Arabidopsis thaliana* (Cunningham et al., 2003; Egert et al., 2013; Sprenger and

467   Keller, 2000; Zhuo et al., 2013; Zuther et al., 2004). The enzymes myo-inositol phosphate synthase

468   (MIPS) and inositol monophosphatase (IMP) are indirectly involved in raffinose synthesis, as they

469   catalyze the *de novo* synthesis of inositol, which is required for the formation of the galactosyl donor

470   galactinol (Saravitz et al., 1987; Sengupta et al., 2015). *MIPS* and *IMP* genes were also shown to be

471   upregulated at low temperatures in plants like rice (*Oryza sativa*), yellow passion fruit (*Passiflora*

472   *ligularis*), or chickpea (*Cicer arietinum*) and have been implicated to play a role in environmental

28

473   stress responses by promoting RFO biosynthesis (Abreu and Aragão, 2007; Kaur et al., 2008; Saxena

474   et al., 2013; R.-X. Zhang et al., 2017).

475   We observed that raffinose synthesis was highly upregulated upon freezing temperatures (**Fig. 5 and**

476   **Table 1**) suggesting a central role for the involved enzymes in sugar beet freezing response. Among

477   the four genes coding for GOLS isoforms in the sugar beet genome (**Table1 and Supplemental**

478   **Figure S5**), three were upregulated upon exposure to freezing, including the two closest homologs to

479   GOLS2 and GOLS3 from Arabidopsis. (**Table 1 and Supplemental Figure S4**). *AtGOLS2* and *AtGOLS3*

480   are both known to be upregulated specifically by drought and cold stress (Maruyama et al., 2009;

481   Shen et al., 2020; Taji et al., 2002) and their induction involves DREB1A/CBF3 transcription factors

482   (Maruyama et al., 2009). These transcription factors are induced during exposure to low

483   temperatures (Gilmour et al., 1998; Shinwari et al., 1998; **Fig. 2H**), and their expression has been

484   shown to confer freezing tolerance in Arabidopsis, rice, or perennial ryegrass (*Lolium perenne*)

485   (Gilmour et al., 2000; Ito et al., 2006; Li et al., 2011).

486   Seven raffinose synthase isoforms were identified in sugar beet, of which two were not differentially

487   regulated upon exposure to low temperatures and three isoforms were differentially regulated in leaf

488   and taproot tissues (**Table1 and Supplemental Figure S4**). The two close homologs of *AtRS2* and

489   *AtRS5* were upregulated at freezing temperatures and showed the most pronounced induction in the

490   freezing tolerant cultivars GT2 and GT3 (**Table 1**). While AtRS2 was shown to possess α-galactosidase

491   activity (Peters et al., 2010), AtRS5 was proven to be a raffinose synthase, upregulated in the cold

492   (Egert et al., 2013). Interestingly, *BvRS5*, the closest homolog to AtRS5, was also highly upregulated

493   in the piths of the two cultivars with higher freezing tolerance, GT2 and GT3, but not in freezing-

494   sensitive GT1 plants (**Fig. 6B**).

495   Upregulation of *MIPS*, *IMP*, *GOLS* and *RS* isoforms went along with high accumulation of inositol,

496   galactinol and raffinose upon exposure to freezing temperatures (**Fig. 4**). Interestingly, raffinose

497   levels in the pith of more cold tolerant genotypes differed from concentrations in the pith of the

498   susceptible genotype – even in the absence of cold (**Fig. 4D**). GT2, the cultivar with the highest

499   freezing tolerance (**Fig. 1A**) and also the highest upregulation of several *GOLS* and *RS* isoforms (**Table**

500   **1**) shows the highest raffinose amounts in the pith region amongst the three genotypes, already at

501   20°C. In GT3, increase in raffinose concentration upon subzero temperatures is highest, most likely

502   mediated by the high upregulation of *RS5* specifically in the pith tissue (**Fig. 6B and Fig. 4D**). In GT1,

503   raffinose concentrations were not altered by freezing temperatures, which is in line with the

504   expression of raffinose synthases, which were not induced in the pith (**Fig. 6B and Fig. 4D**). These

505   data suggest that survival of the pith tissue might be linked to high raffinose concentrations and are

506   in line with previous reports, that showed that raffinose levels were elevated upon cold and freezing

507   temperatures (Koehler et al., 2015; Yue et al., 2015). Such conditions induce the formation of reactive

508   oxygen species (Gechev et al., 2006), which, when accumulating to high levels, can be harmful to the

509   plant, as they can damage membranes (lipid peroxidation), proteins, RNA and DNA molecules

510   (Choudhury et al., 2017). Accumulation of galactinol and raffinose on the other hand, can diminish

511   those harmful effects of ROS. This is because, high levels of these metabolites were shown to stabilize

512   ascorbate and glutathione concentrations, which are involved in detoxification of ROS concentrations

513   (Keller et al., 2021; Nishizawa-Yokoi et al., 2008). Furthermore, galactinol and raffinose show second-

514   order rate constants for detoxification of hydroxyl radicals higher than those of common antioxidants

515   like ascorbate or glutathione (Nishizawa-Yokoi et al., 2008). Although raffinose is synthesized in the

516   cytosol, about 20% of cellular raffinose is located to the chloroplasts and its concentration in plastids

517   is increased even further at low temperatures (Knaupp et al., 2011; Schneider and Keller, 2009). The

518   majority of cellular raffinose is, however, located in the vacuole, reaching about 60% in cold

519   acclimated Arabidopsis plants (Knaupp et al., 2011). In comparison to leaf tissue, taproot tissue does

520   hardly contain any chloroplasts and the vacuole is most likely the major place for raffinose

521   accumulation under low temperatures. There, raffinose might accumulate near the tonoplast together

30

522   with other carbohydrates. Excess cytosolic H_2O_2 that passes through the tonoplast, or H_2O_2

523   originating from superoxide produced by tonoplast-localized NADPH oxidases, could then react with

524   raffinose, similar to the reaction proposed for fructans (Matros et al., 2015; Peshev et al., 2013), to

525   protect the tonoplast from membrane damage via ROS. In addition to its important role in ROS

526   detoxification, RFOs can assist in the osmotic adjustment and thereby maintain cell turgor during

527   water loss due to freezing (ElSayed et al., 2014) and protect the cell against severe damage. The higher

528   raffinose concentrations of the freezing tolerant cultivars GT2 and GT3 in comparison to freezing

529   sensitive GT1, especially in the freezing damage prone pith tissue, hint towards a beneficial

530   contribution of raffinose for freezing protection of this delicate tissue.

531   In Arabidopsis, ICE-CBF/DREB1-regulation is the main low temperature-responsive pathway leading

532   to raffinose accumulation (Janmohammadi et al., 2015) and in our experiments sugar beet *CBF3* was

533   highly expressed at freezing temperature in the pith (**Fig. 2H**). It is tempting to speculate that the

534   regulation of the same pathway might cause an upregulation of specific GOLS and RS isoforms also

535   here in *B. vulgaris*, as the closest sugar beet homologs to *AtGOLS2*, *AtGOLS3* and *AtRS5* all show

536   similarly high upregulation upon freezing temperatures (**Table 1, Supplemental Figure S4**). This

537   suggests that accumulation of galactinol and especially of raffinose is a regulated acclimation reaction

538   of sugar beet plants rather than a result of an altered metabolism in the context of a general stress

539   response.

540   **MATERIAL AND METHODS**

541   **Plant Material and Growth conditions**

542   Three hybrid sugar beet genotypes with contrasting winter-hardiness (GT1, GT2, GT3; KWS SAAT SE,

543   Germany) were used. Plants were germinated and grown on standard soil substrate ED73

544   (Einheitserdwerke Patzer, Germany) with 10% (v/v) sand under a 10 h light/14 h dark cycle, 60%

545 relative humidity, and 110 µmol $m^{-2} s^{-1}$ light intensity. Plants were grown at 20°C for 10 weeks. The

546 plant population was split and one group was transferred to 12°C for one week and 4°C for one to two

547 weeks (one week for ROS and Photosynthesis measurements; two weeks for metabolite

548 measurements and gene expression) afterwards. After 4°C treatment, plants were transferred to -6°C

549 air temperature and were kept there until soil temperature reached 0°C, which took approximately

550 three days (**Figure 1B**). Control plants were kept at 20°C. During harvest, plants were dissected into

551 leaf, pith and storage root tissues, using a kitchen knife. The pith tissue was identified visually from

552 beets halved lengthwise by its peculiar cellular morphology (**Figure 1E and Figure 2**) by eye. Tissue

553 from two different plants was pooled and treated as one independent replicate, with a total of four

554 replicates per genotype and condition, respectively. After harvest, plant material was transferred to

555 liquid nitrogen. Samples used for metabolite analysis were lyophilized in an Alpha 2-4 LD plus freeze-

556 drier (Christ, Osterode am Harz, Germany) for seven days. Sampled material was pulverized using the

557 Retsch MM301 mill (Retsch, Haan, Germany) with a frequency of 30 s^{-1} for 30 seconds.

558 **Survival rate testing**

559 For survival rate testing of different sugar beet genotypes, greenhouse and field experiments were

560 carried out. Therefore, plants were sown out approximately three months before start of the frost

561 period. During experiments it was made sure, that plants were subjected to soil temperatures below

562 0°C. At least two weeks after frost treatment, dead or rotten sugar beets plants were counted and

563 survival rate was calculated. The survival rates monitor mean values of at least two replications in

564 independent years and at different locations.

565 **Chlorophyll Fluorescence Measurements**

566 Photosynthetic activity of three individual plants per genotype was measured using an Imaging-PAM

567 *M-Series*-System (Heinz Walz, Effeltrich, Germany). Plants were placed in the dark for 8 min to deplete

568   the energy of PSII. Capacity of PSII was measured by saturation with 14 cycles of photosynthetically

569   active radiation (76 µmol photons m^{-2} s^{-1}) light-pulses at 0, 50, and 70 s. Recorded fluorescence was

570   used for calculation of effective quantum yield of PSII (Y(II)) and quantum yield of nonphotochemical

571   quenching (Y(NPQ)).

572   **RNASeq analysis**

573   For RNASeq analysis plants were grown according to the growth regime mentioned by Martins

574   Rodrigues et al. 2020. Additionally, RNA extraction and analysis of RNASeq results including

575   statistical analysis was performed as described in Martins Rodrigues et al., 2020 and data was made

576   publicly available as BioProject PRJNA602804. For general overview of RNASeq results annotations

577   were assigned to the corresponding MapMan bincode found in the mapping file named

578   "Ath_AFFY_STv1.1_TRANSCRIPT_CLUSTER_TAIR10_LOCUS". Means over the log2FC over the three

579   independent genotypes were calculated for each bincode for leaf and taproot tissue, containing every

580   log2FC ≠ 0 and without filtering for significant changes.

581   **Expression analysis via RT-qPCR**

582   Expression analysis of selected genes was performed by reverse transcription quantitative PCR (RT-

583   qPCR) using the primers listed in **Supplemental Table S2**. RNA was extracted from homogenized

584   sugar beet tissue using the NucleoSpin(R) RNA Plant Kit (Machery-Nagel, Düren, Germany) according

585   to the manufacturer's guidelines. RNA transcription into cDNA was performed using the qScript cDNA

586   Synthesis Kit (Quantbio, Beverly, USA).

587   **Metabolite extraction**

588   Soluble metabolites were extracted from freeze dried material. Pulverized material was extracted

589   twice 80% EtOH at 80°C for 1h while shaking. Metabolite extracts were combined and vaporized in a

590   vacufuge concentrator (Eppendorf, Hamburg, Germany). Evaporated pellets were resolved in $_{dd}H_2O$.

591   Pellets remaining from extraction were washed with 80% EtOH and $_{dd}H_2O$ for starch isolation. 200µl

592     $_{dd}H_2O$ were added to the pellet and samples were autoclaved for 40 min at 121°C. For hydrolytic

593   cleavage 200µl enzyme mix (5 U α-Amylase; 5 U Amyloglucosidase; 200 mM Sodium-Acetate; pH 4.8)

594   were added to the pellet and incubated at 37°C for four hours. Enzymatic digestion was terminated

595   by heating to 95°C for 10 minutes. After centrifugation the supernatant was used for starch

596   quantification.

597   **Sugar and starch quantification**

598   Sugars (glucose, fructose, sucrose) and hydrolyzed starch concentrations were measured using a

599   NAD^+-coupled enzymatic assay as described by (Stitt et al., 1989).

600   **Ion chromatography measurements**

601   Anions, cations, organic acids, sugar alcohols, galactinol and raffinose were measured in a 761

602   Compact IC system (Metrohm, Herisau, Switzerland). For anion concentration measurements a

603   Metrosep A Supp 4-250/4.0 column and a Metrosep A Supp 4/5 Guard/4.0 guard column (both

604   Metrohm, Herisau, Switzerland) was used. 50mM H_2SO_4 was used as anti-ion and 1,8 mM Na_2CO_3

605   together with 1,7 mM $NaHCO_3$ dissolved in ultrapure water were used as eluent for anion

606   measurement. For determination of cation concentrations, a Metrosep C4 150/4.0 column and a

607   Metrosep C4 Guard/4.0 guard column (both Metrohm, Herisau, Switzerland) were used. The eluent

608   consisted of 2 mM HNO_3 and 1,6 mM dipicolinic acid dissolved in ultrapure water. Organic acids were

609   separated via the Metrosep organic acids 250/7.8 column, a Metrosep Organic Acids Guard/4.6 guard

610   column (both Metrohm, Herisau, Switzerland), with 0,25 mM H_2SO_4 dissolved in ultrapure water used

611   as eluent and 10mM LiCl as anti-ion. Sugar alcohol, raffinose and galactinol quantification was done

612   by ion chromatography on a Metrosep Carb 2 -250/4.0 column using an 871 IC compact device

613   (Metrohm-Switzerland, Herisau, Switzerland) followed by amperometric quantification. NaOH (0.1

614   M) with Sodium acetate (10mM) was used as the mobile phase. For peak analysis the corresponding

615   software Metrodata IC Net 2.3 SR5 by Metrohm (Herisau, Switzerland) was used.

616   **High-performance liquid chromatography measurements**

617   Amino acid concentrations were measured via high performance liquid chromatography in a Dionex

618   (Dionex Softron, Germering, Germany) system, consisting of a Dionex ASI-100 automated sample

619   injector, a Dionex P680 HPLC pump and a Dionex RF2000 fluorescence detector. An AminoPac® PA1

620   column (Dionex Softron, Germering, Germany) was used for separation of amino acids. 0.1 M NaAc, 7

621   mM Triethanolamine pH 5.2 was used as eluent. Samples were prepared for measurement by adding

622   60 µl boric acid buffer (0.2 M; pH 8.8) and 20 µl 6-aminoquinolyl-N-hydroxysuccinimidyl carbamate

623   (3 mg dissolved in 1.5ml Acetonitrile). Samples were vortexed and incubated at 55°C for 10 minutes.

624   Peaks were analyzed using the Chromeleon software (Thermo Fisher Scientific, Waltham,

625   Massachusetts, USA).

626   **Histological staining, microscopy and determination of cell size**

627   Longitudinal- and cross-sections of sugar beet taproot tissue with a thickness of about 0.5 mm were

628   made with the help of a truffle slicer. Sections were analyzed using a Leica MZ 10 F Binocular (Leica

629   Microsystems, Wetzlar, Germany). For histological staining of cell walls, cross sections were stained

630   using a Fuchsine-Chryosidine-Astra Blue (FCA) staining solution (Morphisto, Frankfurt am Main,

631   Germany). Sections were incubated in staining solution for 5 minutes, washed with water and

632   staining was differentiated in 70% ethanol.

633   For tracking of Phloem unloading in the root tissue, CFDA (5(6)-Carboxyfluorescein diacetate) was

634   loaded onto source leaves as described by Mehdi et al., 2019. Briefly, the cuticle of the upper surface

635   of source leaves was gently scratched with smooth sand paper. CFDA was prepared freshly from stock

636 (stock: 10 mg ml^{-1} in acetone), by 1:7 dilution (v/v) with ddH$_2$O and was pipetted on the roughened

637 leaf surface, which was covered with transparent foil to prevent evaporation through the scratched

638 cuticula. CFDA is non-fluorescent, but membrane permeable before the ester bonds are cleaved to

639 yield the green fluorescent CF (carboxyfluorescein), which then is trapped within cells.

640 Approximately 24h after loading to the leaves, cross sections of taproot / pith tissue were cut using a

641 vibratome (125 μm thickness), or by hand, cell walls were (counter-) stained with propidium iodide

642 and signals detected upon excitation with 488 nm on a Leica SP5 confocal microscope. (Leica,

643 Weimar, Germany).

644 Mean sizes of pith- and storage parenchyma cells were measured with ImageJ (Rasband, 1997-2018)

645 using microscope pictures of sugar beet cross-sections. For determination of pith cell size, cells from

646 the middle of the pith were chosen. For each cell type, ten cells of typical appearance were measured

647 per section. Overall, seven cross-sections were analyzed for cell size determination.

648

649 **ROS staining and Antioxidant measurements**

650 H$_2$O$_2$ and O$_2^-$ were detected in longitudinal taproot sections according to (Fryer et al., 2002). Sections

651 were vacuum infiltrated with 5mM DAB-HCl, pH3, or 5mM NBT in 50mM potassium-Phosphate-

652 buffer, pH7.8, for 1 hour and incubated at 4°C overnight until pictures were taken the next day. Total

653 and reduced ascorbate concentrations were measured according to Gillespie and Ainsworth (2007).

654 Freshly harvested and pulverized material was dissolved in 6% TCA and immediately used for

655 colorimetric detection of ascorbate at 525nm after the reaction with α-α-bipyridyl. Oxidized DHA

656 concentration was calculated by subtraction of the reduced ascorbate from the total ascorbate

657 concentration. Total and oxidized glutathione concentrations were measured by the glutathione

658 reductase mediated reduction of 5´5-Dithiobis (-2-Nitrobenzoic acid) (DTNB) at 412nm according to

659 (Queval and Noctor, 2007). Reduced glutathione concentration was calculated by subtraction of the

660 oxidized glutathione from the total glutathione concentration.

661 **Phylogeny**

662

663 Phylogeny of GOLS and RS isoforms was calculated using the www.phylogeny.fr "one-click" mode

664 (Dereeper et al., 2008). For graphical representation, phylogeny analysis from the Phylogeny.fr

665 platform was loaded into FigTree v1.4.4.

666 **Figure preparation**

667

668 Violin plots were generated using BoxPlotR web page (Spitzer et al., 2014). Figures were prepared

669 using Microsoft Excel and Microsoft PowerPoint.

670 **Statistical analyses**

671 Statistical analysis was performed using Origin Version 2018b (OriginLab Corporation, Northampton,

672 MA, USA). PC analysis was performed using MetaboAnalyst 4.0 web server

673 https://www.metaboanalyst.ca/ (Chong and Xia, 2018).

674

675

676

677

678

679

680

681   **SUPPLEMENTAL INFORMATION**

682   **Supplemental Figure S1.** NBT staining of sugar beet taproot sections and antioxidant level of storage

683   parenchyma for ROS detection.

684   **Supplemental Table S1.** Metabolite concentrations of sugar beet leaf, pith and storage parenchyma

685   tissue.

686   **Supplemental Figure S2.** Differences in metabolite profile changes between sugar beet tissues upon

687   a shift in growth temperature from 20°C to 0°C.

688   **Supplemental Figure S3.** Concentrations of starch, glucose, fructose and sucrose in leaf, pith and

689   root tissue under control and freezing temperatures.

690   **Supplemental Figure S4.** Phylogeny of *Beta vulgaris* GOLS and RS isoforms.

691   **Supplemental Table S2.** Oligonucleotides used in this study.

692

693   **ACKNOWLEDGMENTS**

698

699   **CONFLICT OF INTEREST**

700   The authors declare no conflict of interest.

REFERENCES

Abo-Elwafa, S., Abdel-Rahim, H., Abou-Salama, A., and Teama, E. (2006) Sugar beet floral induction and fertility: Effect of vernalization and day-length extension. *Sugar Tech*. 8: 281–287.

Abreu, E.F., and Aragão, F.J. (2007) Isolation and characterization of a myo-inositol-1-phosphate synthase gene from yellow passion fruit (Passiflora edulis f. flavicarpa) expressed during seed development and environmental stress. *Annals of Botany*. 99: 285–292.

Anchordoguy, T.J., Rudolph, A.S., Carpenter, J.F., and Crowe, J.H. (1987) Modes of interaction of cryoprotectants with membrane phospholipids during freezing. *Cryobiology*. 24: 324–331.

Artschwager, E. (1926) Anatomy of the vegetative organs of the sugar beet. US Government Printing Office.

Barbier, H., Nalin, F., and Guern, J. (1982) Freezing injury in sugar beet root cells: Sucrose leakage and modifications of tonoplast properties. *Plant Science Letters*. 26: 75–81.

Bellin, D., Schulz, B., Soerensen, T.R., Salamini, F., and Schneider, K. (2007) Transcript profiles at different growth stages and tap-root zones identify correlated developmental and metabolic pathways of sugar beet. *J Exp Bot*. 58.

Burke, M., Gusta, L., Quamme, H., Weiser, C., and Li, P. (1976) Freezing and injury in plants. *Annual Review of Plant Physiology*. 27: 507–528.

Chang, D.C., Sohn, H.B., Cho, J.H., Im, J.S., Jin, Y.I., Do, G.R., et al. (2014) Freezing and frost damage of potato plants: a case study on growth recovery, yield response, and quality changes. *Potato Research*. 57: 99–110.

Chen, T., Li, Z., Yin, X., Hu, F., and Hu, C. (2016) Discrimination of genetically modified sugar beets based on terahertz spectroscopy. *Spectrochimica Acta Part A: Molecular and Biomolecular Spectroscopy*. 153: 586–590.

Chong, J., and Xia, J. (2018) MetaboAnalystR: an R package for flexible and reproducible analysis of metabolomics data. *Bioinformatics*. 34: 4313–4314.

Choudhury, F.K., Rivero, R.M., Blumwald, E., and Mittler, R. (2017) Reactive oxygen species, abiotic stress and stress combination. *The Plant Journal*. 90: 856–867.

Cunningham, S., Nadeau, P., Castonguay, Y., Laberge, S., and Volenec, J. (2003) Raffinose and stachyose accumulation, galactinol synthase expression, and winter injury of contrasting alfalfa germplasms. *Crop Science*. 43: 562–570.

De Roover, J., Vandenbranden, K., Van Laere, A., and Van den Ende, W. (2000) Drought induces fructan synthesis and 1-SST (sucrose: sucrose fructosyltransferase) in roots and leaves of chicory seedlings (Cichorium intybus L.). *Planta*. 210: 808–814.

Dereeper, A., Guignon, V., Blanc, G., Audic, S., Buffet, S., Chevenet, F., et al. (2008) Phylogeny. fr: robust phylogenetic analysis for the non-specialist. *Nucleic acids research*. 36: W465–W469.

Dohm, J.C., Minoche, A.E., Holtgräwe, D., Capella-Gutiérrez, S., Zakrzewski, F., Tafer, H., et al. (2013) The genome of the recently domesticated crop plant sugar beet (Beta vulgaris). *Nature*. 505: 546.

Donahue, J.L., Alford, S.R., Torabinejad, J., Kerwin, R.E., Nourbakhsh, A., Ray, W.K., et al. (2010) The Arabidopsis thaliana myo-inositol 1-phosphate synthase1 gene is required for myo-inositol synthesis and suppression of cell death. *The Plant Cell*. 22: 888–903.

Egert, A., Keller, F., and Peters, S. (2013) Abiotic stress-induced accumulation of raffinose in Arabidopsis leaves is mediated by a single raffinose synthase (RS5, At5g40390). *BMC Plant Biology*. 13: 1–9.

ElSayed, A.I., Rafudeen, M.S., and Golldack, D. (2014) Physiological aspects of raffinose family oligosaccharides in plants: protection against abiotic stress. *Plant Biology*. 16: 1–8.

Fanucchi, F., Alpi, E., Olivieri, S., Cannistraci, C.V., Bachi, A., Alpi, A., et al. (2012) Acclimation increases freezing stress response of Arabidopsis thaliana at proteome level. *Biochimica et Biophysica Acta (BBA)-Proteins and Proteomics*. 1824: 813–825.

Fennell, A. (2004) Freezing tolerance and injury in grapevines. *Journal of Crop Improvement*. 10: 201–235.

Fowler, S., and Thomashow, M.F. (2002) Arabidopsis transcriptome profiling indicates that multiple regulatory pathways are activated during cold acclimation in addition to the CBF cold response pathway. *The Plant Cell*. 14: 1675–1690.

Fryer, M.J., Oxborough, K., Mullineaux, P.M., and Baker, N.R. (2002) Imaging of photo-oxidative stress responses in leaves. *Journal of experimental botany*. 53: 1249–1254.

Ganter, C., Böck, A., Buckel, P., and Mattes, R. (1988) Production of thermostable, recombinant α-galactosidase suitable for raffinose elimination from sugar beet syrup. *Journal of Biotechnology*. 8: 301–310.

Gechev, T.S., Van Breusegem, F., Stone, J.M., Denev, I., and Laloi, C. (2006) Reactive oxygen species as signals that modulate plant stress responses and programmed cell death. *Bioessays*. 28: 1091–1101.

Giaquinta, R.T. (1979) Sucrose translocation and storage in the sugar beet. *Plant Physiol*. 63.

Gillespie, K.M., and Ainsworth, E.A. (2007) Measurement of reduced, oxidized and total ascorbate content in plants. *Nature Protocols*. 2: 871–874.

Gilmour, S.J., Sebolt, A.M., Salazar, M.P., Everard, J.D., and Thomashow, M.F. (2000) Overexpression of the Arabidopsis CBF3transcriptional activator mimics multiple biochemical changes associated with cold acclimation. *Plant physiology*. 124: 1854–1865.

Gilmour, S.J., Zarka, D.G., Stockinger, E.J., Salazar, M.P., Houghton, J.M., and Thomashow, M.F. (1998) Low temperature regulation of the Arabidopsis CBF family of AP2 transcriptional activators as an early step in cold-induced COR gene expression. *The Plant Journal*. 16: 433–442.

Guy, C.L. (1990) Cold acclimation and freezing stress tolerance: role of protein metabolism. *Annual review of plant biology*. 41: 187–223.

Haagenson, D.M., Klotz, K.L., and Campbell, L. (2008) Impact of storage temperature, storage duration, and harvest date on sugarbeet raffinose metabolism. *Postharvest biology and technology*. 49: 221–228.

Hincha, D.K., Livingston III, D.P., Premakumar, R., Zuther, E., Obel, N., Cacela, C., et al. (2007) Fructans from oat and rye: composition and effects on membrane stability during drying. *Biochimica et Biophysica Acta (BBA)-Biomembranes*. 1768: 1611–1619.

Ho, L.-H., Rode, R., Siegel, M., Reinhardt, F., Neuhaus, H.E., Yvin, J.-C., et al. (2020) Potassium Application Boosts Photosynthesis and Sorbitol Biosynthesis and Accelerates Cold Acclimation of Common Plantain (Plantago major L.). *Plants*. 9: 1259.

Hoffmann, C.M., and Kluge-Severin, S. (2011) Growth analysis of autumn and spring sown sugar beet. *European Journal of Agronomy*. 34: 1–9.

Ito, Y., Katsura, K., Maruyama, K., Taji, T., Kobayashi, M., Seki, M., et al. (2006) Functional analysis of rice DREB1/CBF-type transcription factors involved in cold-responsive gene expression in transgenic rice. *Plant and Cell Physiology*. 47: 141–153.

Jaggard, K., Qi, A., and Ober, E. (2009) Capture and use of solar radiation, water, and nitrogen by sugar beet (Beta vulgaris L.). *Journal of experimental botany*. 60: 1919–1925.

Jahnke, S., Menzel, M.I., Van Dusschoten, D., Roeb, G.W., Bühler, J., Minwuyelet, S., et al. (2009) Combined MRI–PET dissects dynamic changes in plant structures and functions. *The Plant Journal*. 59: 634–644.

799 Janmohammadi, M., Zolla, L., and Rinalducci, S. (2015) Low temperature tolerance in plants:
800   changes at the protein level. *Phytochemistry*. 117: 76–89.
801 Kaur, H., Shukla, R.K., Yadav, G., Chattopadhyay, D., and Majee, M. (2008) Two divergent
802   genes encoding L-myo-inositol 1-phosphate synthase1 (CaMIPS1) and 2 (CaMIPS2) are
803   differentially expressed in chickpea. *Plant, Cell & Environment*. 31: 1701–1716.
804 Keller, I., Rodrigues, C.M., Neuhaus, H.E., and Pommerrenig, B. (2021) Improved resource
805   allocation and stabilization of yield under abiotic stress. *Journal of Plant Physiology*. 257:
806   153336.
807 Klemens, P.A.W., Patzke, K., Trentmann, O., Poschet, G., Büttner, M., Schulz, A., et al. (2014)
808   Overexpression of a proton-coupled vacuolar glucose exporter impairs freezing tolerance
809   and seed germination. *New Phytologist*. 202: 188–197.
810 Knaupp, M., Mishra, K.B., Nedbal, L., and Heyer, A.G. (2011) Evidence for a role of raffinose in
811   stabilizing photosystem II during freeze–thaw cycles. *Planta*. 234: 477–486.
812 Knoblauch, M., Vendrell, M., de Leau, E., Paterlini, A., Knox, K., Ross-Elliot, T., et al. (2015)
813   Multispectral Phloem-Mobile Probes: Properties and Applications. *Plant Physiol*. 167:
814   1211.
815 Kockelmann, A., Tilcher, R., and Fischer, U. (2010) Seed production and processing. *Sugar*
816   *Tech*. 12: 267–275.
817 Koehler, G., Rohloff, J., Wilson, R.C., Kopka, J., Erban, A., Winge, P., et al. (2015) Integrative
818   "omic" analysis reveals distinctive cold responses in leaves and roots of strawberry,
819   Fragaria× ananassa 'Korona'. *Frontiers in plant science*. 6: 826.
820 Li, T., Zhang, Y., Liu, Y., Li, X., Hao, G., Han, Q., et al. (2020) Raffinose synthase enhances
821   drought tolerance through raffinose synthesis or galactinol hydrolysis in maize and
822   Arabidopsis plants. *Journal of Biological Chemistry*. 295: 8064–8077.
823 Li, X., Cheng, X., Liu, J., Zeng, H., Han, L., and Tang, W. (2011) Heterologous expression of the
824   Arabidopsis DREB1A/CBF3 gene enhances drought and freezing tolerance in transgenic
825   Lolium perenne plants. *Plant Biotechnology Reports*. 5: 61–69.
826 Liu, Y., Dang, P., Liu, L., and He, C. (2019) Cold acclimation by the CBF–COR pathway in a
827   changing climate: Lessons from Arabidopsis thaliana. *Plant cell reports*. 38: 511–519.
828 Loel, J., and Hoffmann, C. (2015) Relevance of osmotic and frost protecting compounds for the
829   winter hardiness of autumn sown sugar beet. *Journal of Agronomy and Crop Science*.
830   201: 301–311.
831 Loewus, F.A., and Murthy, P.P. (2000) myo-Inositol metabolism in plants. *Plant science*. 150: 1–
832   19.
833 Maqbool, A., Shafiq, S., and Lake, L. (2010) Radiant frost tolerance in pulse crops—a review.
834   *Euphytica*. 172: 1–12.
835 Maruyama, K., Takeda, M., Kidokoro, S., Yamada, K., Sakuma, Y., Urano, K., et al. (2009)
836   Metabolic pathways involved in cold acclimation identified by integrated analysis of
837   metabolites and transcripts regulated by DREB1A and DREB2A. *Plant physiology*. 150:
838   1972–1980.
839 Matros, A., Peshev, D., Peukert, M., Mock, H., and Van den Ende, W. (2015) Sugars as hydroxyl
840   radical scavengers: proof-of-concept by studying the fate of sucralose in Arabidopsis.
841   *The Plant Journal*. 82: 822–839.
842 Mehdi, R., Lamm, C.E., Bodampalli Anjanappa, R., Müdsam, C., Saeed, M., Klima, J., et al.
843   (2019) Symplasmic phloem unloading and radial post-phloem transport via vascular rays
844   in tuberous roots of Manihot esculenta. *Journal of experimental botany*. 70: 5559–5573.
845 Metzner, R., van Dusschoten, D., Bühler, J., Schurr, U., and Jahnke, S. (2014) Belowground
846   plant development measured with magnetic resonance imaging (MRI): exploiting the
847   potential for non-invasive trait quantification using sugar beet as a proxy. *Frontiers in*
848   *plant science*. 5: 469.

849 Milford, G., and Riley, J. (1980) The effects of temperature on leaf growth of sugar beet
850   varieties. *Annals of Applied Biology*. 94: 431–443.
851 Moliterni, V.M.C., Paris, R., Onofri, C., Orrù, L., Cattivelli, L., Pacifico, D., et al. (2015) Early
852   transcriptional changes in Beta vulgaris in response to low temperature. *Planta*. 242:
853   187–201.
854 Nishizawa, A., Yabuta, Y., and Shigeoka, S. (2008) Galactinol and raffinose constitute a novel
855   function to protect plants from oxidative damage. *Plant physiology*. 147: 1251–1263.
856 Nishizawa-Yokoi, A., Yabuta, Y., and Shigeoka, S. (2008) The contribution of carbohydrates
857   including raffinose family oligosaccharides and sugar alcohols to protection of plant cells
858   from oxidative damage. *Plant signaling & behavior*. 3: 1016–1018.
859 Pennycooke, J.C., Jones, M.L., and Stushnoff, C. (2003) Down-regulating α-galactosidase
860   enhances freezing tolerance in transgenic petunia. *Plant Physiology*. 133: 901–909.
861 Peshev, D., Vergauwen, R., Moglia, A., Hideg, É., and Van den Ende, W. (2013) Towards
862   understanding vacuolar antioxidant mechanisms: a role for fructans? *Journal of
863   Experimental Botany*. 64: 1025–1038.
864 Peters, S., Egert, A., Stieger, B., and Keller, F. (2010) Functional identification of Arabidopsis
865   ATSIP2 (At3g57520) as an alkaline α-galactosidase with a substrate specificity for
866   raffinose and an apparent sink-specific expression pattern. *Plant and cell physiology*. 51:
867   1815–1819.
868 Peters, S., and Keller, F. (2009) Frost tolerance in excised leaves of the common bugle (Ajuga
869   reptans L.) correlates positively with the concentrations of raffinose family
870   oligosaccharides (RFOs). *Plant, Cell & Environment*. 32: 1099–1107.
871 Pommerrenig, B., Cvetkovic, J., Trentmann, O., Klemens, P.A.W., Neuhaus, H.E., and Ludewig,
872   F. (2018) In Concert: Orchestrated Changes in Carbohydrate Homeostasis Are Critical
873   for Plant Abiotic Stress Tolerance. *Plant and Cell Physiology*. 59: 1290–1299.
874 Pommerrenig, B., Müdsam, C., Kischka, D., and Neuhaus, H.E. (2020) Treat and Trick:
875   Common Regulation and Manipulation of Sugar Transporters During Sink Establishment
876   by the Plant and the Invader. *Journal of Experimental Botany*.
877 Pontis, H. (1989) Fructans and cold stress. *Journal of Plant Physiology*. 134: 148–150.
878 Queval, G., and Noctor, G. (2007) A plate reader method for the measurement of NAD, NADP,
879   glutathione, and ascorbate in tissue extracts: application to redox profiling during
880   Arabidopsis rosette development. *Analytical biochemistry*. 363: 58–69.
881 Rodrigues, C.M., Müdsam, C., Keller, I., Zierer, W., Czarnecki, O., Corral, J.M., et al. (2020)
882   Vernalization Alters Sink and Source Identities and Reverses Phloem Translocation from
883   Taproots to Shoots in Sugar Beet (Beta vulgaris). *The Plant Cell*.
884 Saito, M., and Yoshida, M. (2011) Expression analysis of the gene family associated with
885   raffinose accumulation in rice seedlings under cold stress. *Journal of plant physiology*.
886   168: 2268–2271.
887 Saravitz, D.M., Pharr, D.M., and Carter, T.E. (1987) Galactinol synthase activity and soluble
888   sugars in developing seeds of four soybean genotypes. *Plant physiology*. 83: 185–189.
889 Saxena, S.C., Salvi, P., Kaur, H., Verma, P., Petla, B.P., Rao, V., et al. (2013) Differentially
890   expressed myo-inositol monophosphatase gene (CaIMP) in chickpea (Cicer arietinum L.)
891   encodes a lithium-sensitive phosphatase enzyme with broad substrate specificity and
892   improves seed germination and seedling growth under abiotic stresses. *Journal of
893   experimental botany*. 64: 5623–5639.
894 Schneider, T., and Keller, F. (2009) Raffinose in chloroplasts is synthesized in the cytosol and
895   transported across the chloroplast envelope. *Plant and Cell Physiology*. 50: 2174–2182.
896 Sengupta, S., Mukherjee, S., Basak, P., and Majumder, A.L. (2015) Significance of galactinol
897   and raffinose family oligosaccharide synthesis in plants. *Frontiers in plant science*. 6:
898   656.

899   Shen, Y., Jia, B., Wang, J., Cai, X., Hu, B., Wang, Y., et al. (2020) Functional analysis of
900   Arabidopsis thaliana galactinol synthase AtGolS2 in response to abiotic stress. *Molecular*
901   *Plant Breeding*. 11.
902   Shinwari, Z.K., Nakashima, K., Miura, S., Kasuga, M., Seki, M., Yamaguchi-Shinozaki, K., et al.
903   (1998) An Arabidopsis gene family encoding DRE/CRT binding proteins involved in low-
904   temperature-responsive gene expression. *Biochemical and biophysical research*
905   *communications*. 250: 161–170.
906   Spitzer, M., Wildenhain, J., Rappsilber, J., and Tyers, M. (2014) BoxPlotR: a web tool for
907   generation of box plots. *Nature methods*. 11: 121.
908   Sprenger, N., and Keller, F. (2000) Allocation of raffinose family oligosaccharides to transport
909   and storage pools in Ajuga reptans: the roles of two distinct galactinol synthases. *The*
910   *Plant Journal*. 21: 249–258.
911   Stitt, M., Lilley, R.McC., Gerhardt, R., and Heldt, H.W. (1989) [32] Metabolite levels in specific
912   cells and subcellular compartments of plant leaves. In *Methods in Enzymology*. pp. 518–
913   552 Academic Press.
914   Strand, Å., Hurry, V., Gustafsson, P., and Gardeström, P. (1997) Development of Arabidopsis
915   thaliana leaves at low temperatures releases the suppression of photosynthesis and
916   photosynthetic gene expression despite the accumulation of soluble carbohydrates. *The*
917   *Plant Journal*. 12: 605–614.
918   Taji, T., Ohsumi, C., Iuchi, S., Seki, M., Kasuga, M., Kobayashi, M., et al. (2002) Important roles
919   of drought-and cold-inducible genes for galactinol synthase in stress tolerance in
920   Arabidopsis thaliana. *The Plant Journal*. 29: 417–426.
921   Thomashow, M.F. (1999) Plant cold acclimation: freezing tolerance genes and regulatory
922   mechanisms. *Annual review of plant biology*. 50: 571–599.
923   Turesson, H., Andersson, M., Marttila, S., Thulin, I., and Hofvander, P. (2014) Starch
924   biosynthetic genes and enzymes are expressed and active in the absence of starch
925   accumulation in sugar beet tap-root. *BMC Plant Biology*. 14: 104.
926   Usadel, B., Blaesing, O.E., Gibon, Y., Poree, F., Hoehne, M., Guenter, M., et al. (2008)
927   Multilevel genomic analysis of the response of transcripts, enzyme activities and
928   metabolites in Arabidopsis rosettes to a progressive decrease of temperature in the non-
929   freezing range. *Plant, Cell & Environment*. 31: 518–547.
930   Wolfe, J., and Bryant, G. (1999) Freezing, Drying, and/or Vitrification of Membrane– Solute–
931   Water Systems. *Cryobiology*. 39: 103–129.
932   Wyse, R., and Dexter, S. (1971) Effect of agronomic and storage practices on raffinose,
933   reducing sugar, and amino acid content of sugarbeet varieties. *J Am Soc Sugar Beet*
934   *Technol*. 16: 369–383.
935   Yadav, S.K. (2010) Cold stress tolerance mechanisms in plants. A review. *Agronomy for*
936   *sustainable development*. 30: 515–527.
937   Yue, C., Cao, H.-L., Wang, L., Zhou, Y.-H., Huang, Y.-T., Hao, X.-Y., et al. (2015) Effects of cold
938   acclimation on sugar metabolism and sugar-related gene expression in tea plant during
939   the winter season. *Plant molecular biology*. 88: 591–608.
940   Zhang, R.-X., Qin, L.-J., and Zhao, D.-G. (2017) Overexpression of the OsIMP gene increases
941   the accumulation of inositol and confers enhanced cold tolerance in tobacco through
942   modulation of the antioxidant enzymes' activities. *Genes*. 8: 179.
943   Zhang, Y.-F., Li, G.-L., Wang, X.-F., Sun, Y.-Q., and Zhang, S.-Y. (2017) Transcriptomic profiling
944   of taproot growth and sucrose accumulation in sugar beet (Beta vulgaris L.) at different
945   developmental stages. *PloS one*. 12: e0175454.
946   Zhuo, C., Wang, T., Lu, S., Zhao, Y., Li, X., and Guo, Z. (2013) A cold responsive galactinol
947   synthase gene from Medicago falcata (MfGolS1) is induced by myo-inositol and confers
948   multiple tolerances to abiotic stresses. *Physiologia plantarum*. 149: 67–78.

949   Zuther, E., Büchel, K., Hundertmark, M., Stitt, M., Hincha, D.K., and Heyer, A.G. (2004) The role
950   of raffinose in the cold acclimation response of Arabidopsis thaliana. *Febs Letters.* 576:
951   169–173.

952